Fundamental Studies of SOFC Materials

Eric D. Wachsman

University of Florida - U.S. Department of Energy
High Temperature Electrochemistry Center

Department of Materials Science and Engineering
University of Florida

ewach@mse.ufl.edu
http://hitec.mse.ufl.edu

QuickTime™ and a
GIF decompressor
are needed to see this picture.

UF-DOE HiTEC

Highlights of:

Determination of Electrochemical Performance and Thermo-Mechanical-Chemical Stability of SOFCs from Defect Modeling

DOE SECA Contract No: DE-FC26-02NT41562

DOE Project Manager: Travis Schultz

- Advance the fundamental understanding of the continuum-level electrochemistry of oxide mixed ionic-electronic conductors.
- Obtain fundamental constants required for implementing the continuum-level electrochemical model from experiment.
- Extend the models to multilayer structures and incorporate microstructural effects.
- Verify the models through experiment.
- Develop a transient version of the continuum-level electrochemical model.
- Obtain time constants for various transport processes from electrical impedance spectroscopy to examine the effects of transients on SOFC performance.
- Develop and deliver software modules for incorporation of the continuum-level electrochemical model into SOFC failure analysis software used by NETL, PNNL, ORNL and the SECA industrial teams.

Electrocatalytically Active High Surface Area Cathodes for Low Temperature SOFCs

DOE EE/FE Contract No: DE-FC26-03NT41959

DOE Project Manager: Lane Wilson

- Develop a fundamental understanding of heterogeneous electrocatalytic phenomena at the surface of ion conducting ceramics.
- Fabricate high surface area SOFC cathodes with controlled microstructure and porosity.
- Develop low ASR cathodes for low to intermediate temperature SOFCs.

UF - DOE High Temperature Electrochemistry Center

DOE Advanced Research, HiTEC Contract No: DE-AC05-76RL01830

DOE Project Manager: Lane Wilson

- Develop the fundamental understanding of ionic transport in, and electrocatalytic phenomena on the surface of, ion conducting materials, spanning the range from first-principles calculations and molecular dynamic simulations of ionic transport and gas-solid interactions to synthesis and characterization of novel ion conducting materials and electrocatalysts.

FUNDAMENTAL PROPERTIES

DEFECT STRUCTURE

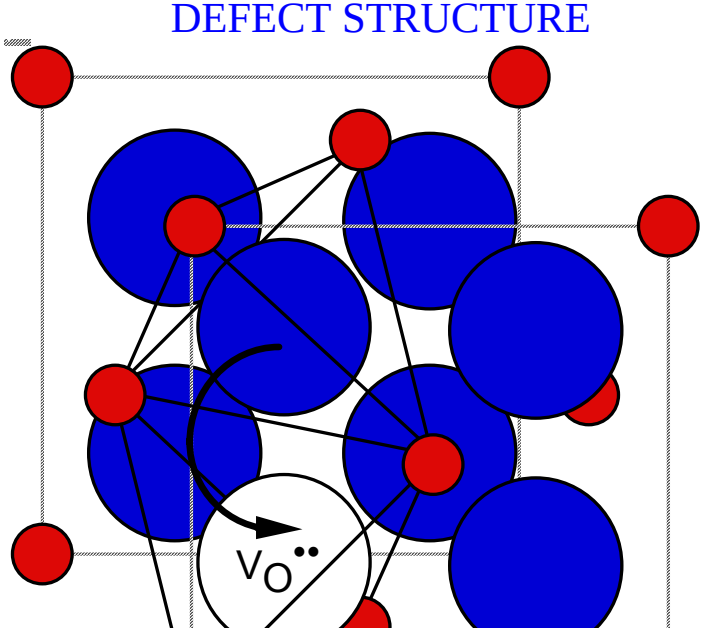

DEFECT EQUILIBRIA

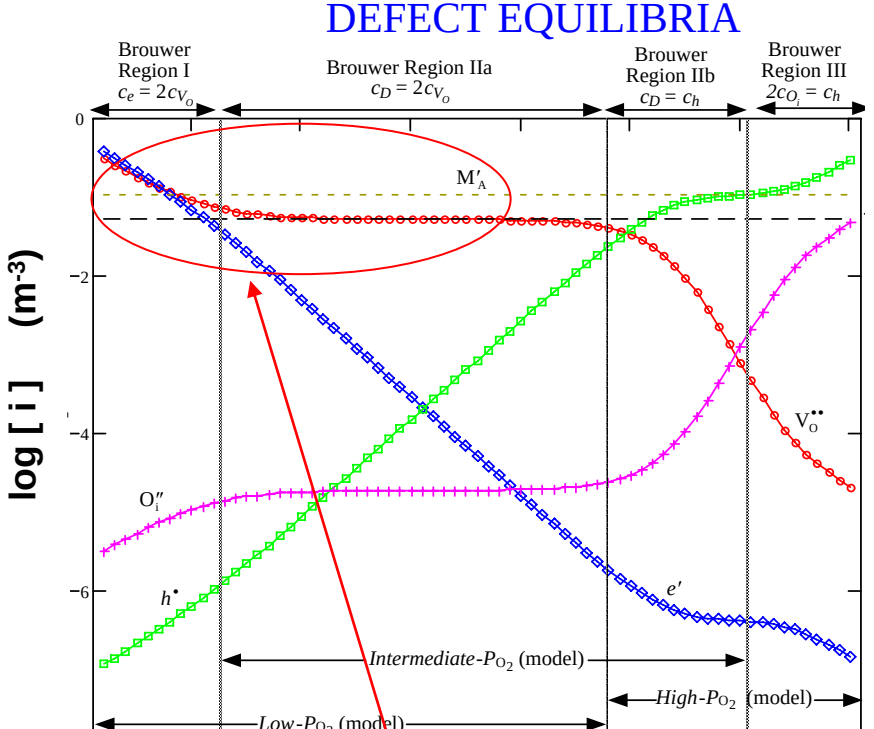

Defect Energetics and Mobility Based on:

- Crystal structure
- Cation radii
- Cation polarizability
- Cation oxidation state
- Etc.

Defect Concentration Dependence on:

- Defect formation energy
- Temperature
- P_{O2}

$$c_V = \left[\frac{3}{4}K_r^{\frac{1}{2}}P_{O_2}^{-\frac{1}{4}} + \left(\frac{A}{2}\right)^{\frac{3}{2}}\right]^{\frac{2}{3}}$$

EXTENSION OF MODEL TO THERMO-MECHANICAL PROPERTIES

QuickTime™ and a
TIFF (LZW) decompressor
are needed to see this picture.

$$E_{bond} = \frac{A}{r^m} - \frac{B}{r^n}$$

A, B, n and m are constants

Thermal expansion

$$\frac{a - a_0}{a_0} = \alpha \Delta T$$

Chemical expansion

$$\frac{a - a_0}{a_0} = \frac{\theta}{a_0} c_V$$

Thermo - chemical expansion

$$\frac{a - a_0}{a_0} = \alpha \Delta T + \frac{\theta}{a_0} c_V$$

Lattice constant, a, has linear relationship with c_v

Therefore, $r \sim a \sim c_v$

$$c_V = \left[\frac{3}{4} K_r^{\frac{1}{2}} P_{O_2}^{-\frac{1}{4}} + \left(\frac{A}{2} \right)^{\frac{3}{2}} \right]^{\frac{2}{3}}$$

Thermo-Chemical Expansion of GDC

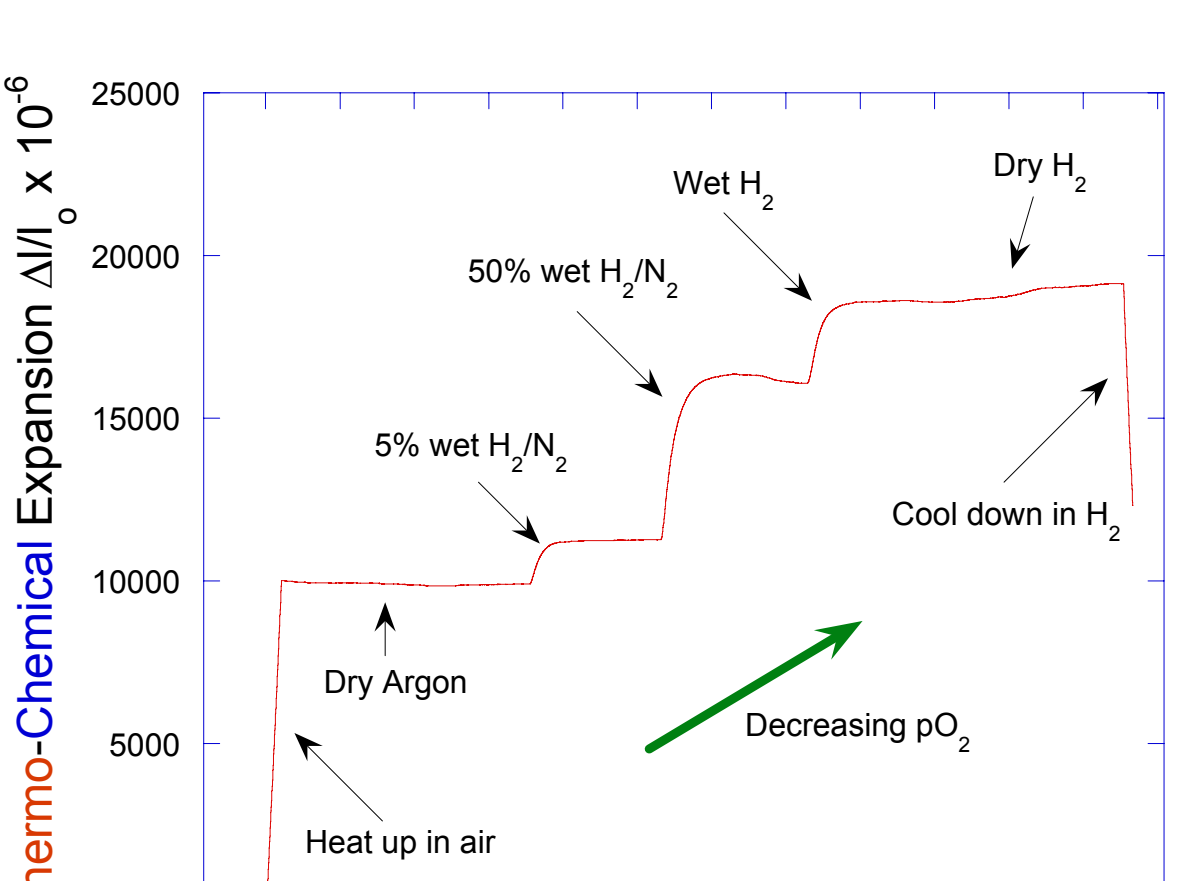

EXTENSION OF MODEL TO THERMO-MECHANICAL PROPERTIES

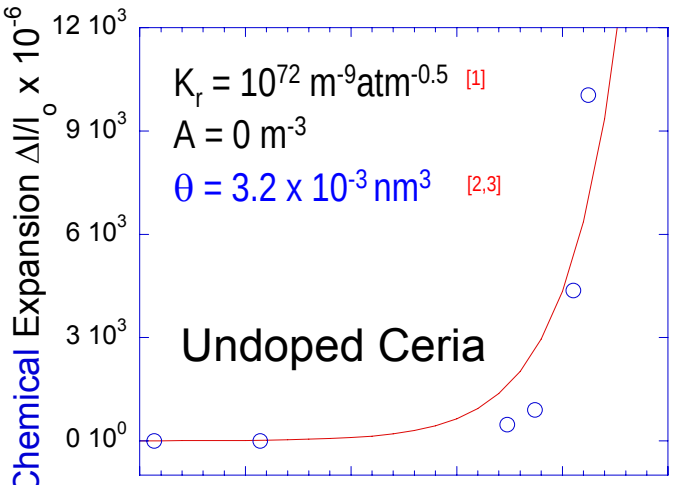

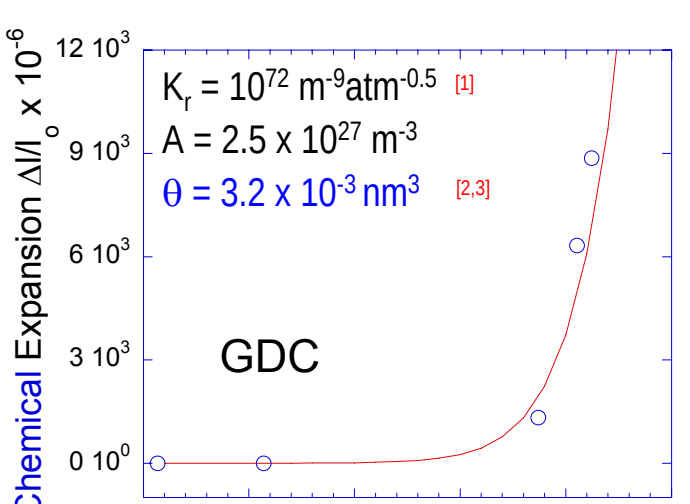

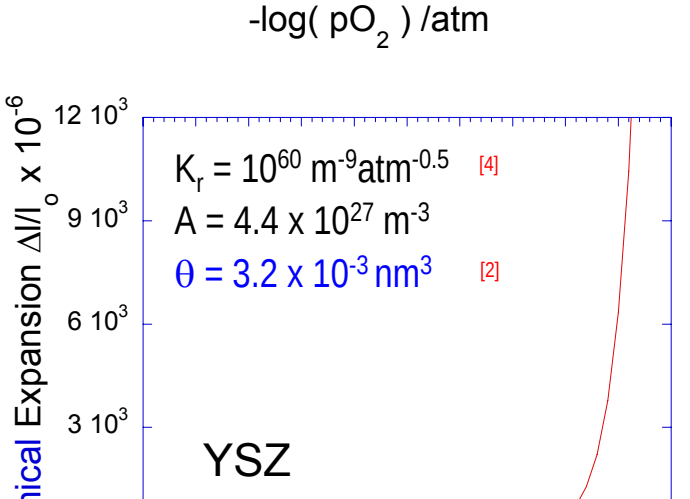

$$\frac{\Delta l}{l_0} = \underbrace{\alpha \Delta T}_{\text{thermal}} + \underbrace{\theta\left(\tfrac{3}{4} K_R^{\frac{1}{2}} P_{O_2}^{-\frac{1}{4}} + \left(\tfrac{1}{2} A\right)^{\frac{3}{2}}\right)^{\frac{2}{3}}}_{\text{chemical}}$$

1. T. Kobayashi et al., Solid State Ionics, 126 (1999) 349
2. D.J. Kim, J. Am. Ceram. Soc., 72 (1989) 1415
3. M. Mogensen et al., Solid State Ionics, 129 (2000) 63
4. K. Sasaki and J. Maier, Solid State Ionics, 134 (2000) 303

EXTENSION OF MODEL TO THERMO-MECHANICAL PROPERTIES

QuickTime™ and a
TIFF (LZW) decompressor
are needed to see this picture.

$$E_{bond} = \frac{A}{r^m} - \frac{B}{r^n}$$

A, B, n and m are constants

$$Y_{bond} = \frac{1}{r_0}\left(\frac{d^2E}{dr^2}\right)_{r=r_0}$$

$$\frac{Y}{Y^*} \approx \left(\frac{a}{a_0}\right)^{-(\delta+3)}$$

$$\frac{a}{a_0} = \theta c_V + 1$$

$$Y \approx Y^*\left(\theta c_V + 1\right)^{-(\delta+3)}$$

Lattice constant, a, has linear relationship with c_v

Therefore, $r \sim a \sim c_V$

δ is equivalent to:

- n (if A is constant)
- m (if B is constant)

as oxygen vacancies are introduced

1. *D-J. Kim, J. Amer. Ceram. Soc. 72 (1989) 1415.*
2. *M. Mogensen, N. Sammes, G. Tompsett, Solid State Ionics 129 (2000) 63*

EXTENSION OF MODEL TO THERMO-MECHANICAL PROPERTIES
Experimental Validation

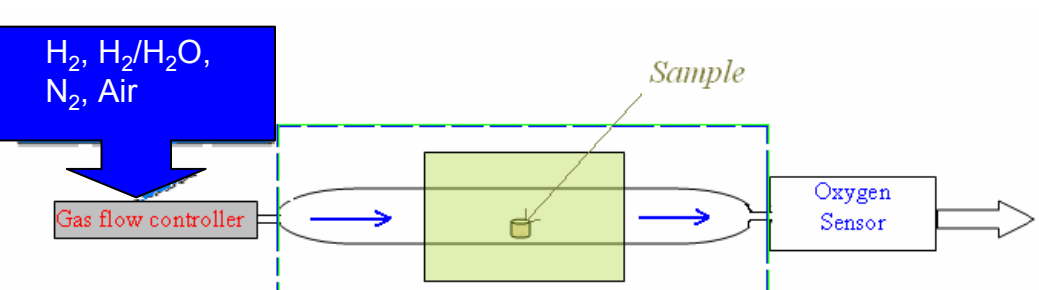

PO_2= 0.22 atm

PO_2=9.5x10^{-5} atm

PO_2=1.8x10^{-17} atm

PO_2=4.5x10^{-22} atm

PO_2=5.1x10^{-25} atm

P_{O2}

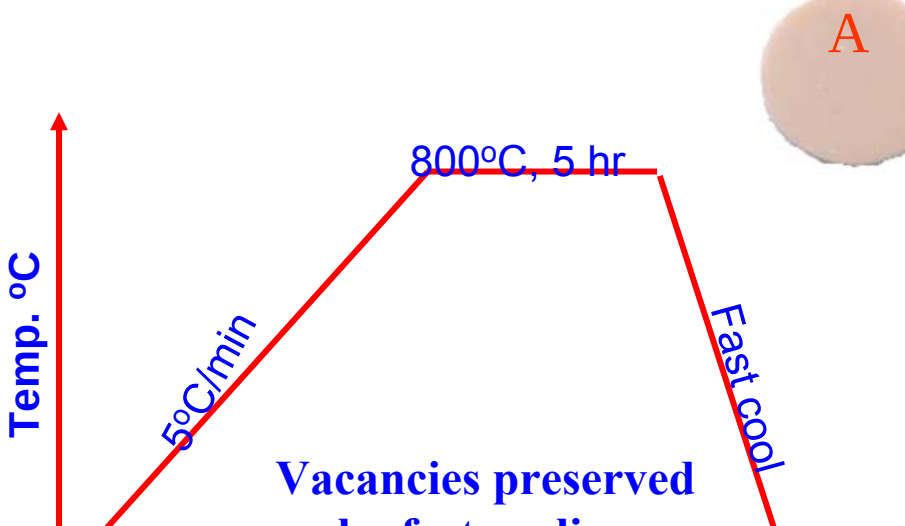

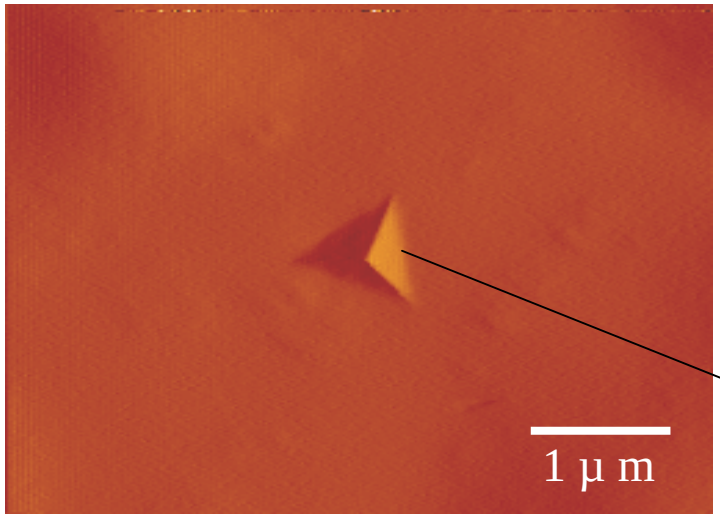

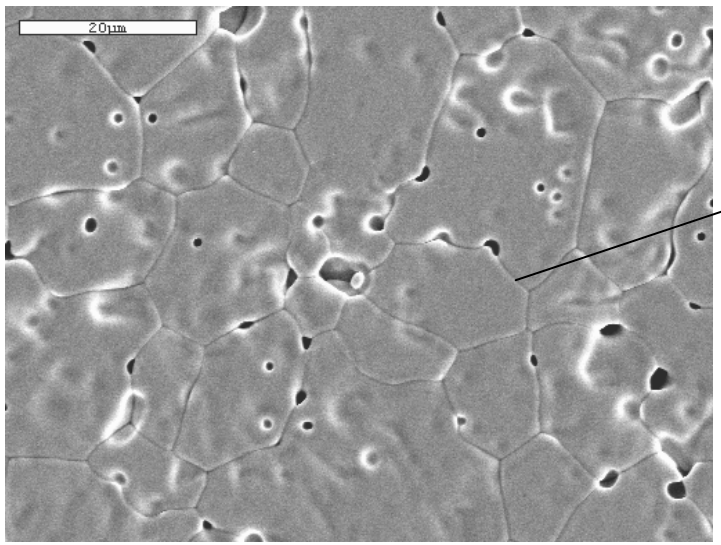

SEM image of surface after thermal etch.
Average grain size ~12 µm.

Nanoindents

Size: **~0.6 µm**

Depth: **~125 nm**

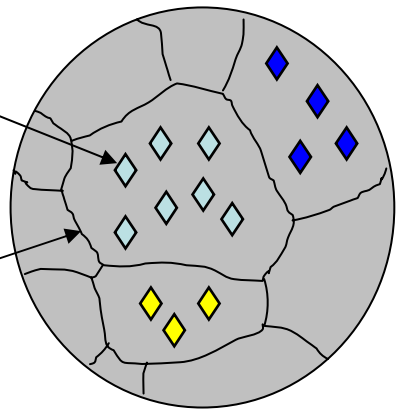

•Effect of crystallographic orientation on elastic modulus and hardness evaluated statistically by applying many indents on grains of known orientation.

•In-plane anisotropy can be measured by changing the indent orientation.

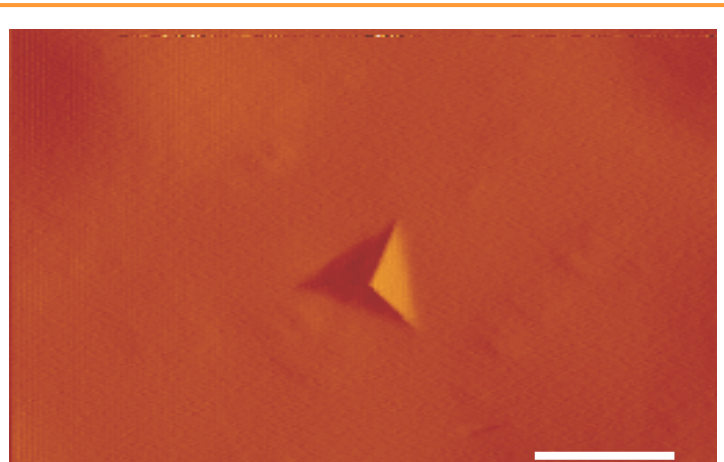

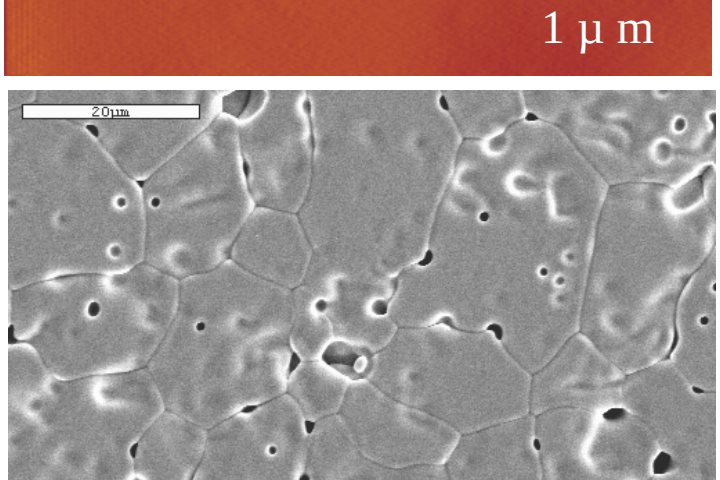

SEM image of surface after thermal etch.
Average grain size ~12 µm.

Nanoindents

Size: **~0.6 µm**

Depth: **~125 nm**

- **100 indents were applied on the sample, which covered 100 µm X 100 µm (~25 different grains)**

Modulus: 218.35±11.12 GPa

Hardness: 9.00±0.73 Gpa

- **The small variations imply that ceria is elastically isotropic.**

Effect of Oxygen Vacancy Population on Elastic Modulus of

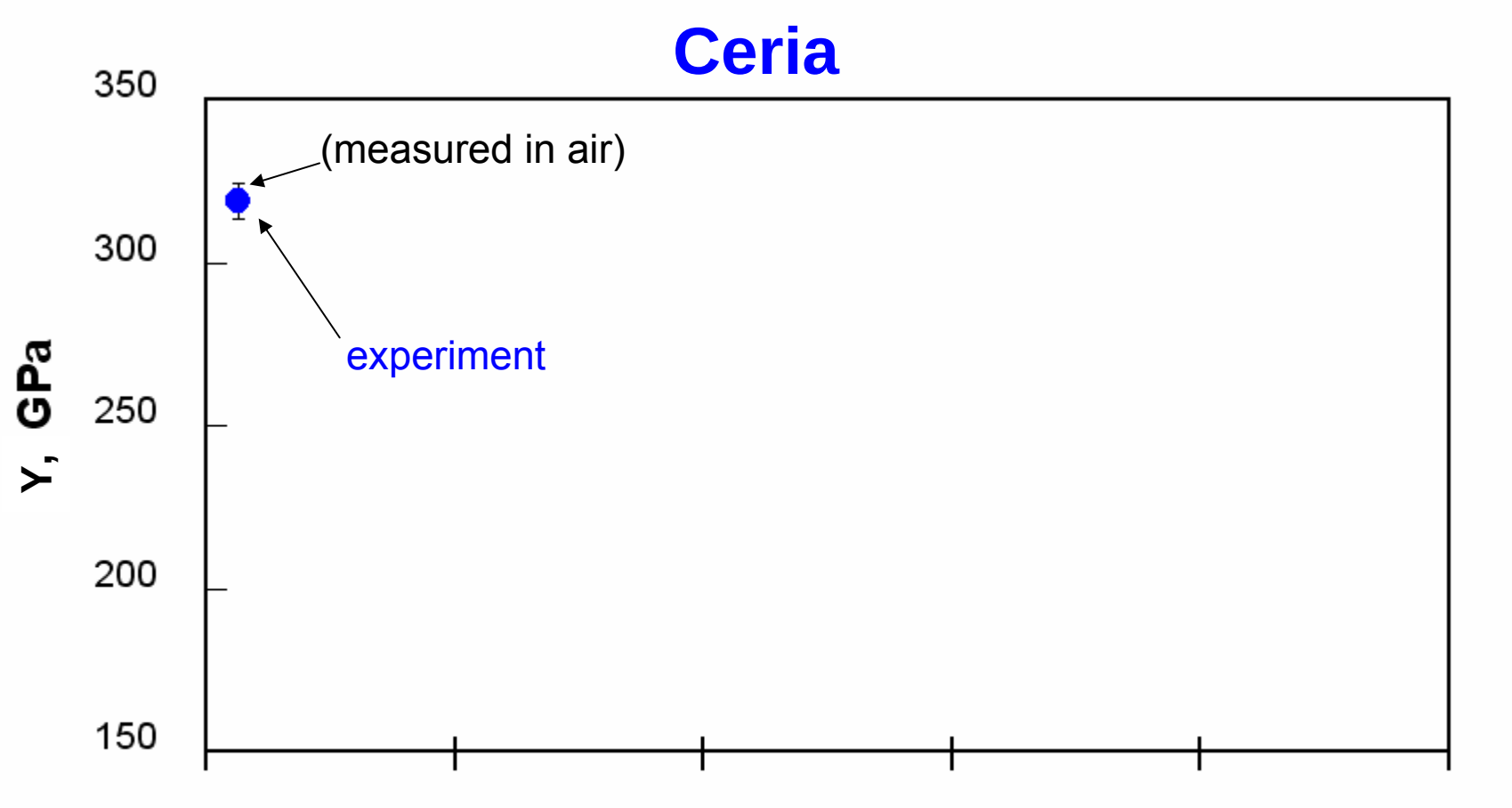

Effect of Oxygen Vacancy Population on Elastic Modulus of

Ceria

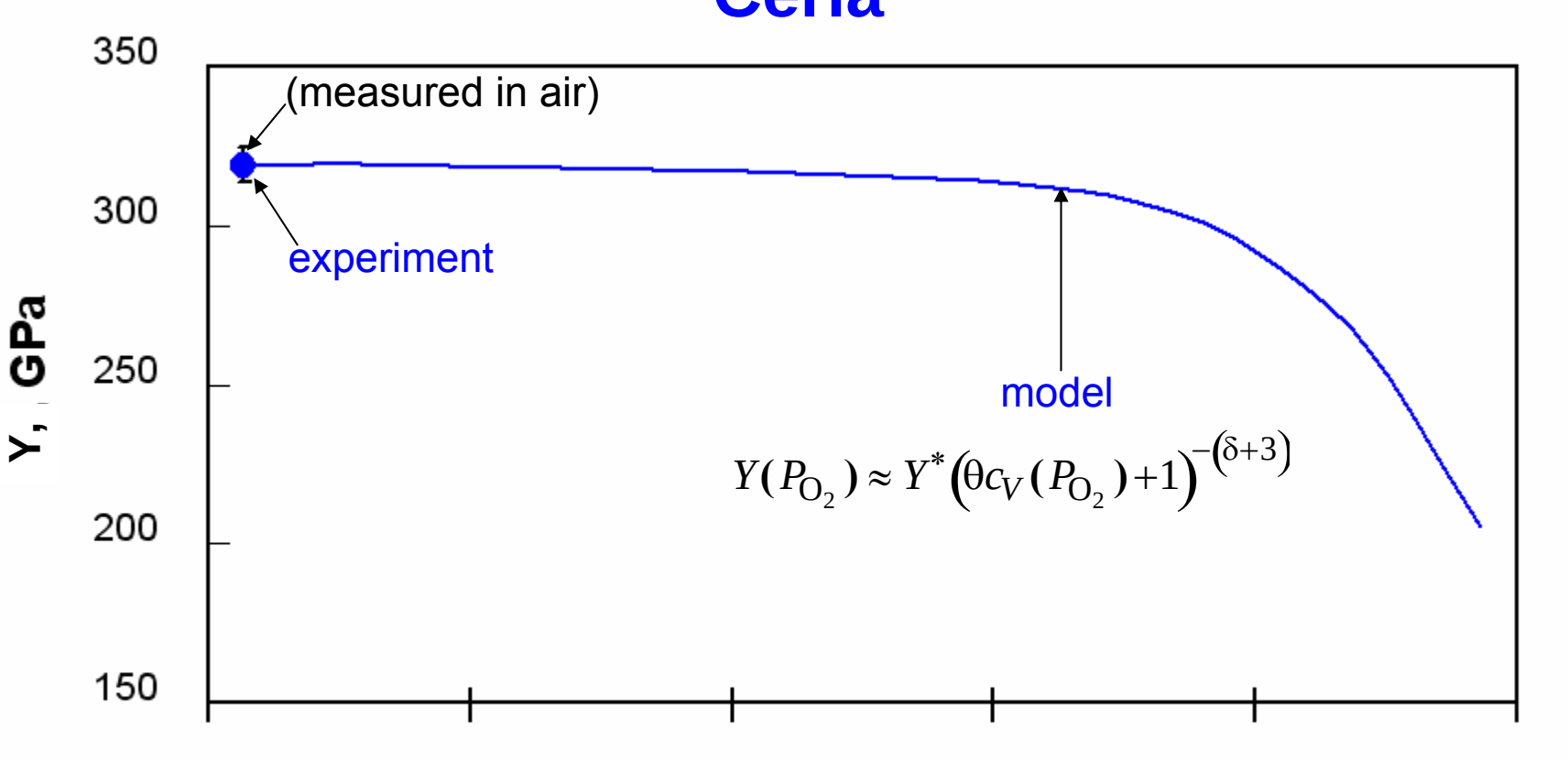

Effect of Oxygen Vacancy Population on Elastic Modulus of

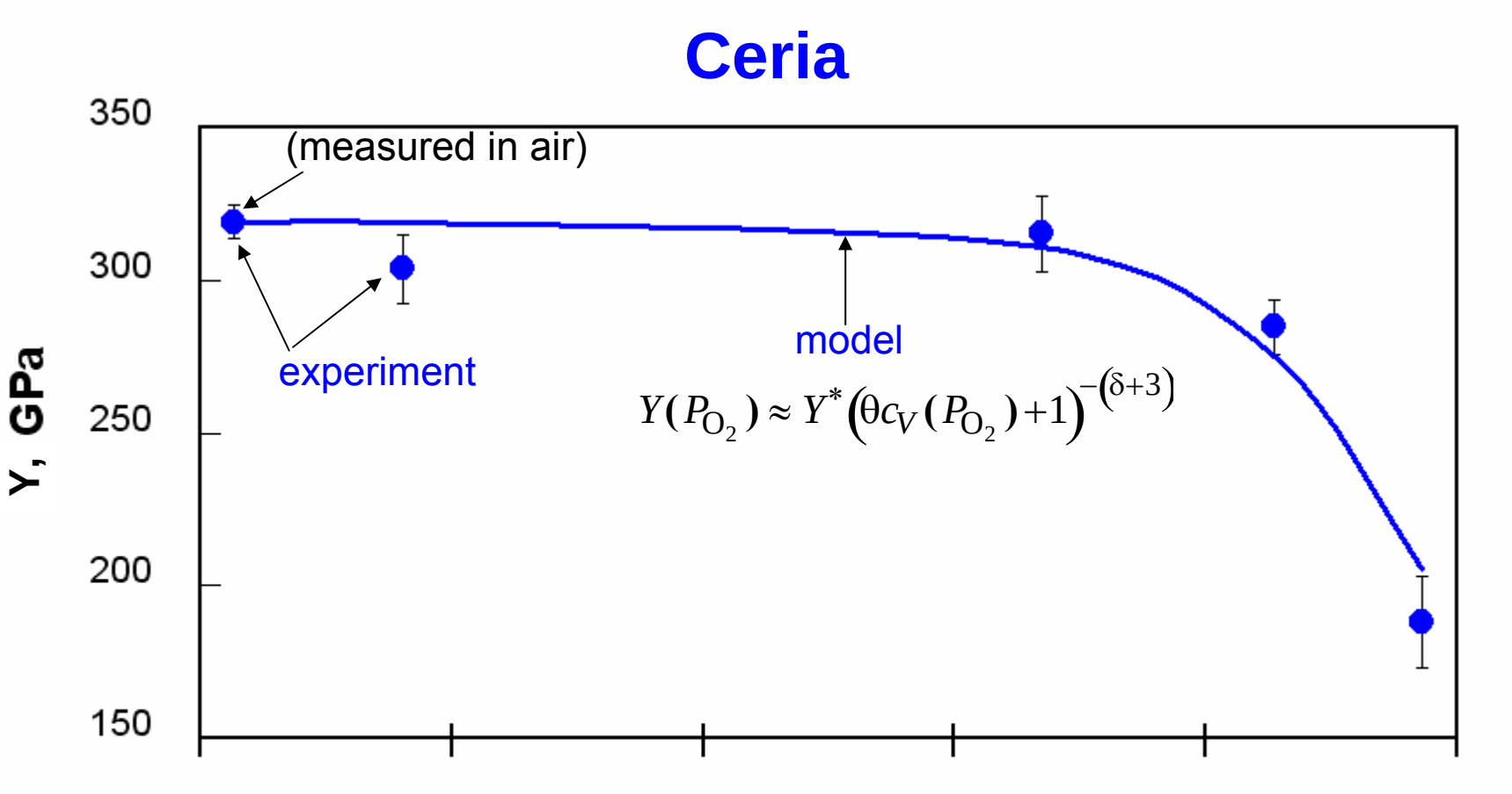

Effect of Oxygen Vacancy Population on Elastic Modulus of

Gadolinia-Doped Ceria (GDC)

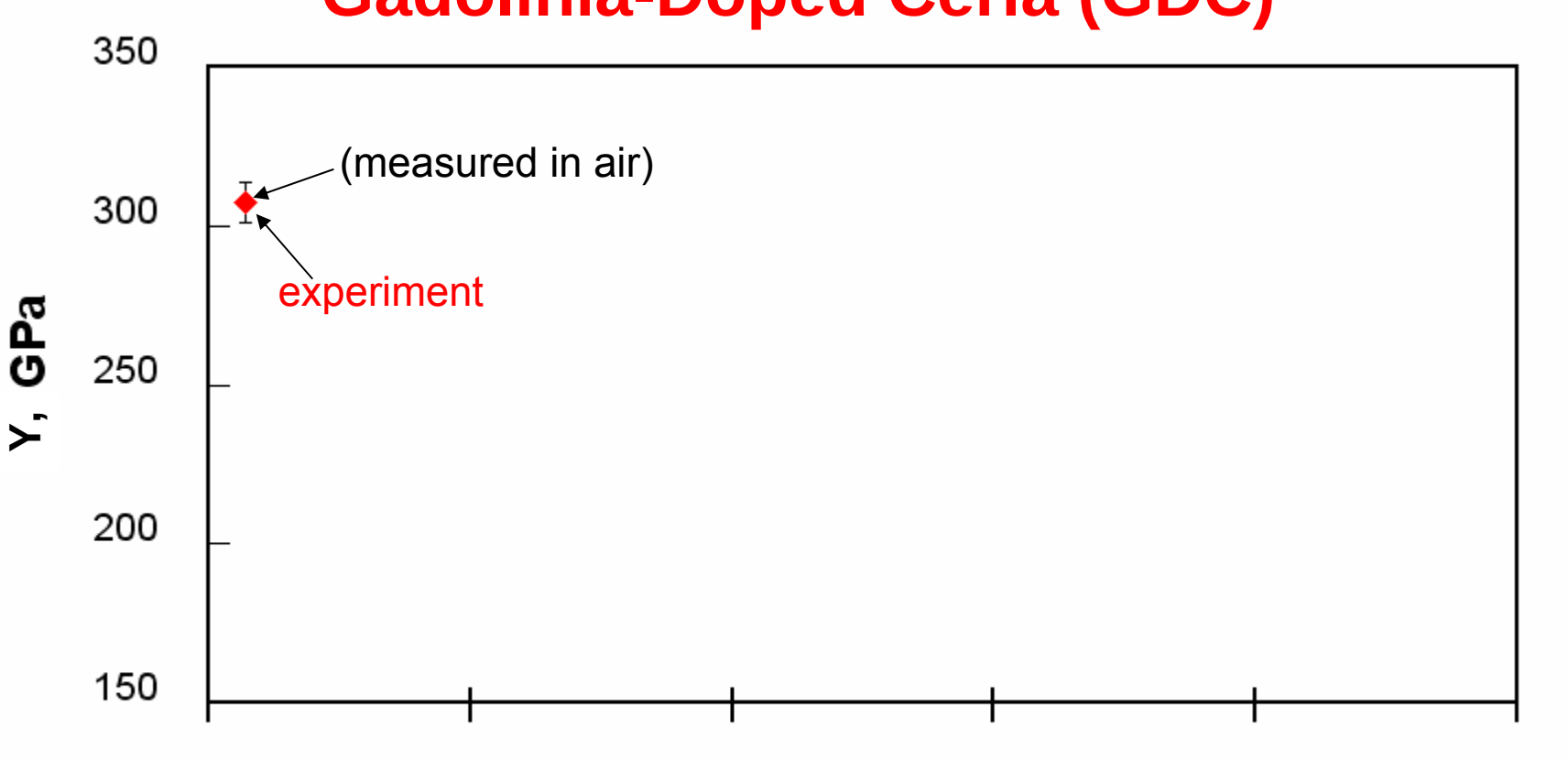

Effect of Oxygen Vacancy Population on Elastic Modulus of

Gadolinia-Doped Ceria (GDC)

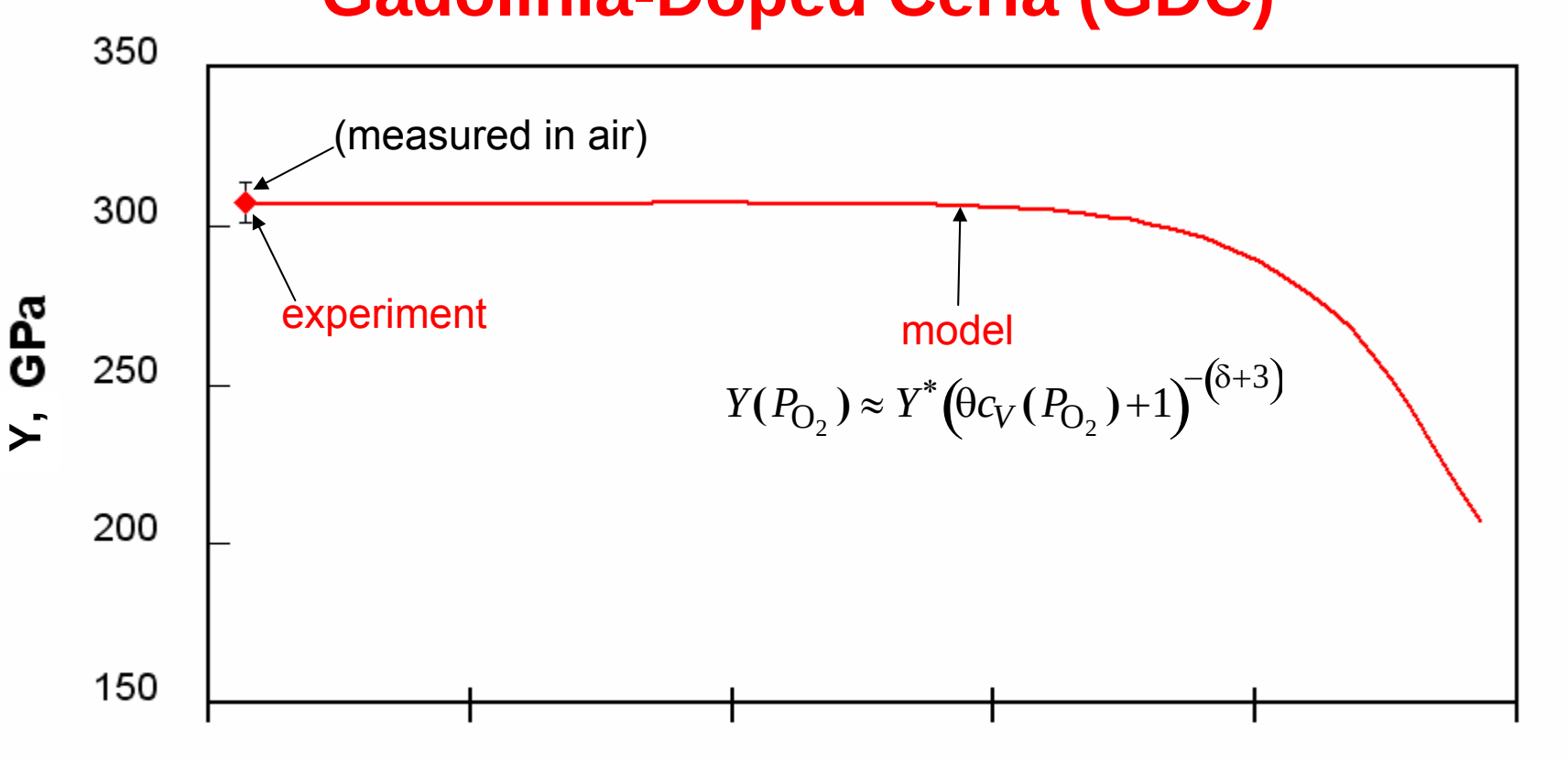

Effect of Oxygen Vacancy Population on Elastic Modulus of

Gadolinia-Doped Ceria (GDC)

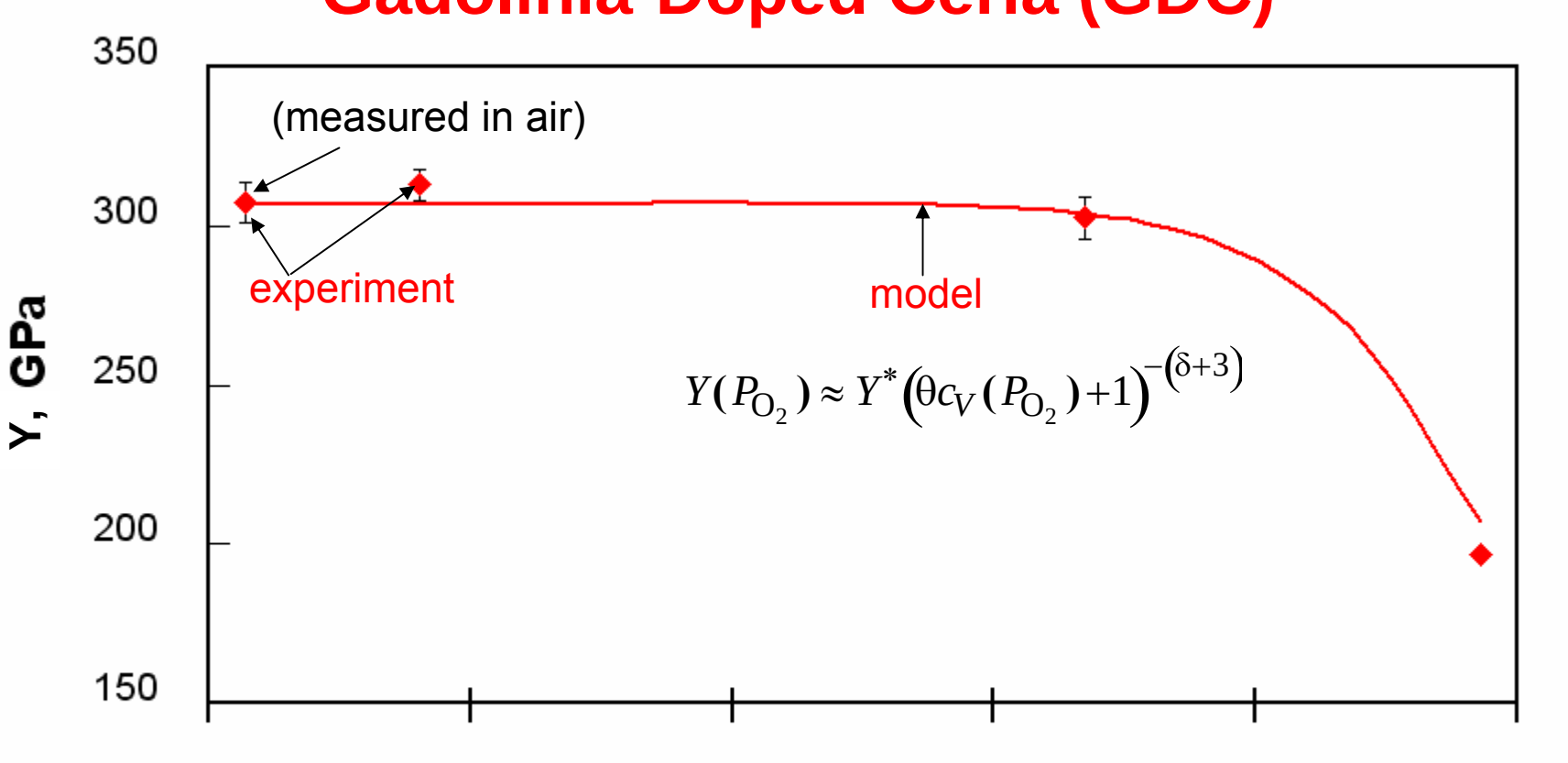

Effect of Oxygen Vacancy Population on Elastic Modulus of

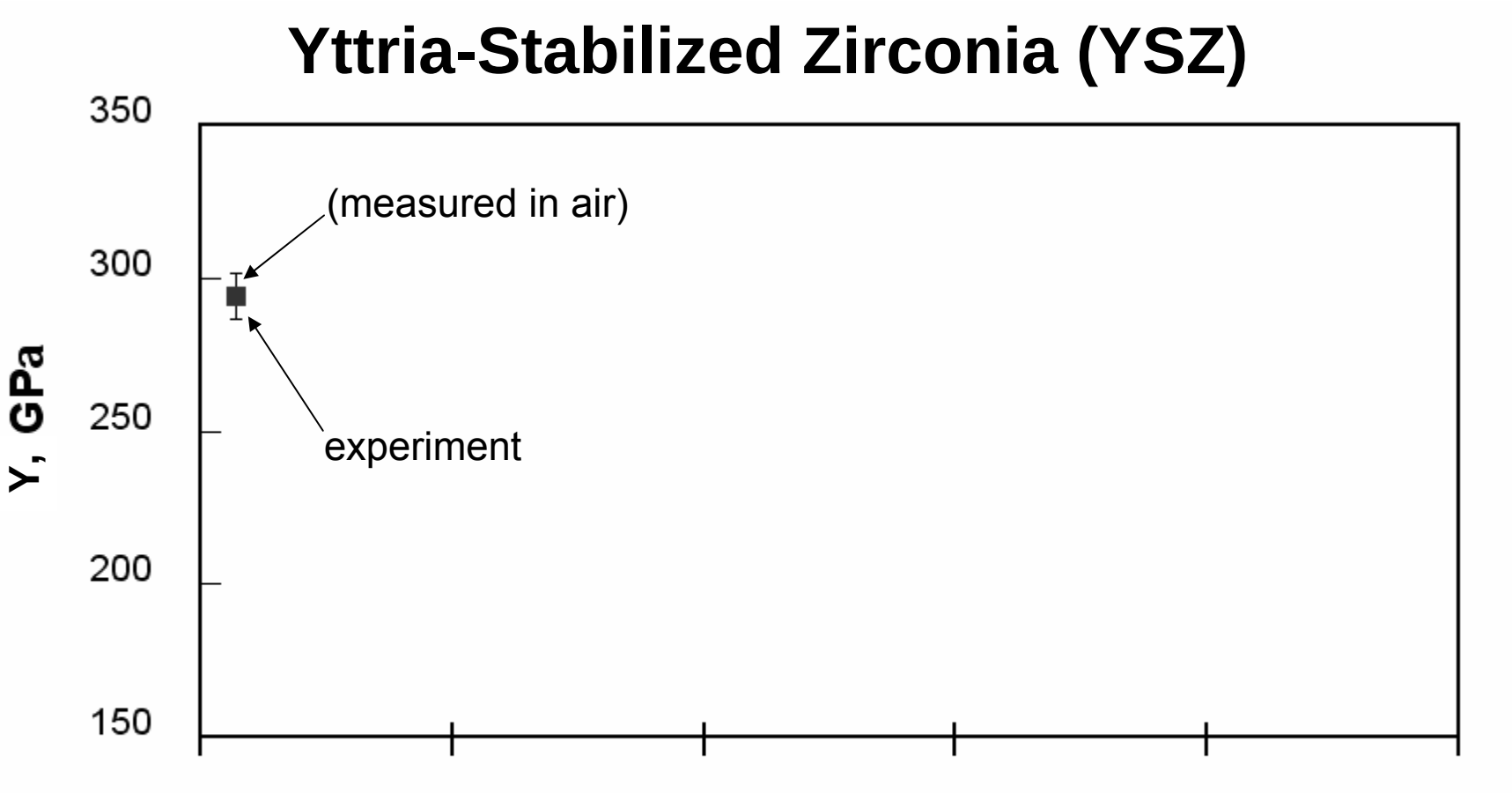

Effect of Oxygen Vacancy Population on Elastic Modulus of

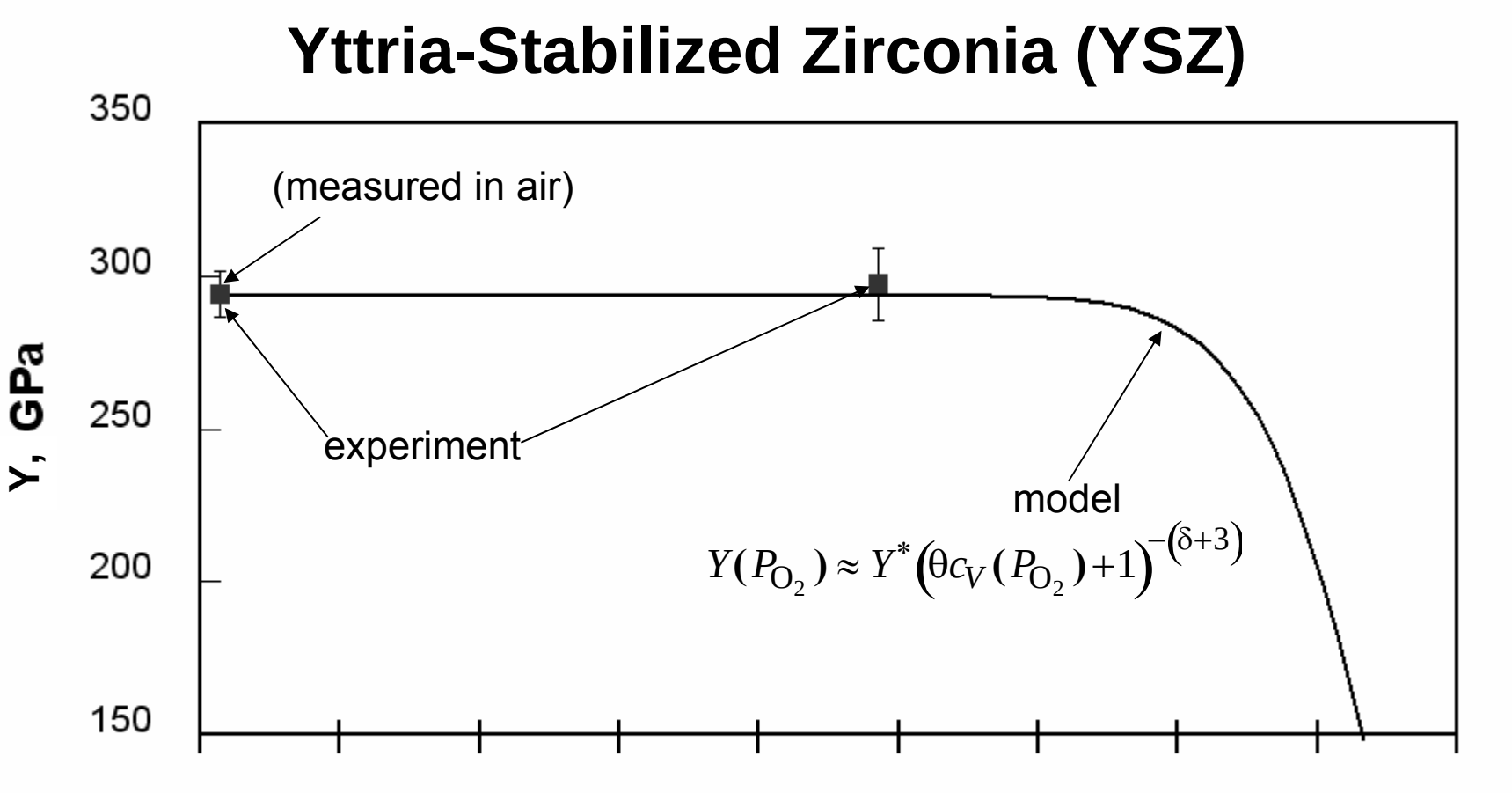

Higher temperature and higher current will shift decrease in modulus to higher P_{O2}

Effect of Oxygen Vacancy Population on Elastic Modulus of

Ceria, GDC,YSZ

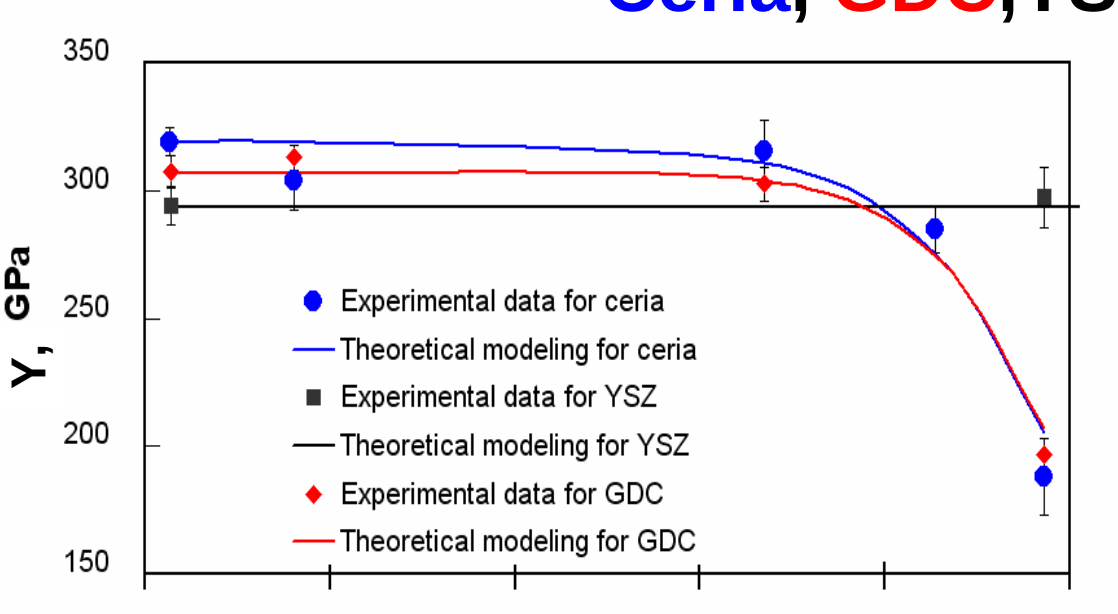

$$Y(P_{O_2}) \approx Y^*\left(\theta c_V(P_{O_2})+1\right)^{-(\delta+3)}$$

Extend to Include Microstructural Effects:

$Y(p) = Y_{p=0}(1-p)^r$ where p is porosity and r ≈ 2 for porous ceramics [1]

$$Y(P_{O_2}, p) = Y^*(\theta c_V(P_{O_2})+1)^{-(\delta+3)}(1-p)^r$$

1. A. S. Wagh, R. B. Poepel, J. P. Singh, J. Mat. Sci., **26** (1991) 3862.

EXTENSION OF MODEL TO THERMO-MECHANICAL PROPERTIES

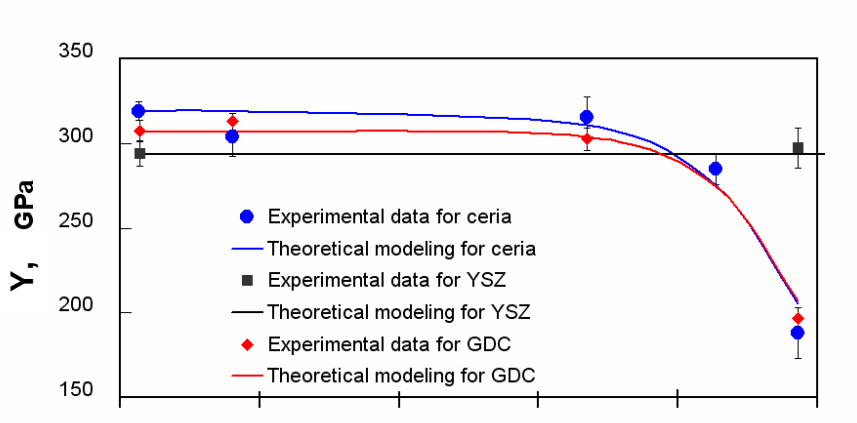

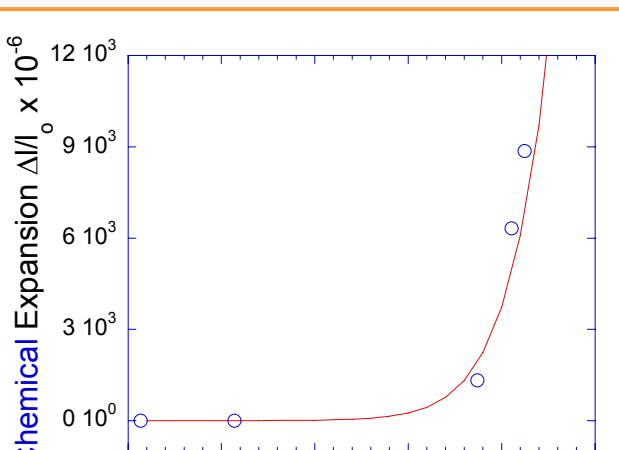

$$Y(P_{O_2}) \approx Y^{*}\left(\underbrace{\theta\left(\tfrac{3}{4}K_R^{\frac{1}{2}}P_{O_2}^{-\frac{1}{4}}+\left(\tfrac{1}{2}A\right)^{\frac{3}{2}}\right)^{\frac{2}{3}}}_{\text{chemical}}+1\right)^{-(\delta+3)}$$

$$\frac{\Delta l}{l_0}=\underbrace{\alpha\Delta T}_{\text{thermal}}+\underbrace{\theta\left(\tfrac{3}{4}K_R^{\frac{1}{2}}P_{O_2}^{-\frac{1}{4}}+\left(\tfrac{1}{2}A\right)^{\frac{3}{2}}\right)^{\frac{2}{3}}}_{\text{chemical}}$$

SAME!

K_R = Equilibrium constant for $V_O^{\bullet\bullet}$ formation

A = Dopant concentration

θ = Empirical constant = 3.2 x 10^{-3} nm^3 [1,2]

1. *D-J. Kim, J. Amer. Ceram. Soc. 72 (1989) 1415.*
2. *M. Mogensen, N. Sammes, G. Tompsett, Solid State Ionics 129 (2000) 63*

FUNDAMENTAL QUANTITATIVE DEFECT CONSTANTS

K_R

Thermodynamics of Oxides

- Computational and experimental thermodynamics of SOFC materials.

Equilibrium constant for $V_O^{\bullet\bullet}$ formation

$$O_O^X = V_O^{\bullet\bullet} + 2e' + 1/2O_2$$

$$K_R = [V_O^{\bullet\bullet}]\, n^2\, P_{O2}^{0.5}/[O_O^X]$$

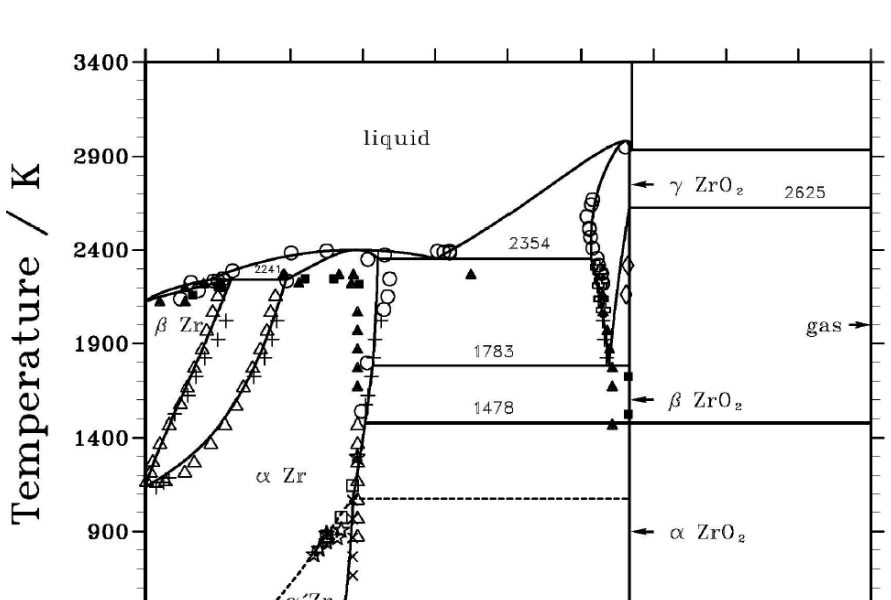

Calculated Zr-O phase diagram

FUNDAMENTAL QUANTITATIVE DEFECT CONSTANTS

$$\theta = ?$$

Computational Materials Thrust

- Large-scale molecular dynamics simulations to elucidate the effects ionic radius and polarizability of on ionic conductivity, the structure of vacancy clusters, and the mechanisms of oxygen transport.
- First principles, electronic structure simulations. Calculation of defect formation energy in oxides from first principles and thermodynamics. Study of oxygen reactions at surfaces and interfaces.

QuickTime™ and a
TIFF (LZW) decompressor
are needed to see this picture.

$$E_{bond} = \frac{A}{r^m} - \frac{B}{r^n}$$

A, B, n and m are constants

FUNDAMENTAL QUANTITATIVE DEFECT CONSTANTS

$\theta = ?$

Computational Materials Thrust

- Large-scale molecular dynamics simulations to elucidate the effects ionic radius and polarizability of on ionic conductivity, the structure of vacancy clusters, and the mechanisms of oxygen transport.
- First principles, electronic structure simulations. Calculation of defect formation energy in oxides from first principles and thermodynamics. Study of oxygen reactions at surfaces and interfaces.

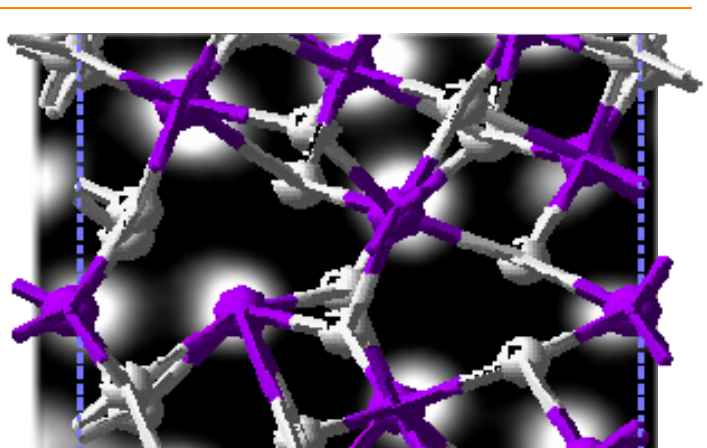

Ab-initio calculation of ZrO_2 grain boundary and comparison with Z-contrast TEM image

V_O^x

$V_O^{\cdot}$

QuickTime™ and a TIFF (LZW) decompressor are needed to see this picture.

$V_O^{\cdot\cdot}$

Defect formation energies as a function of P_{O2}

FUNDAMENTAL PROPERTIES

DEFECT STRUCTURE

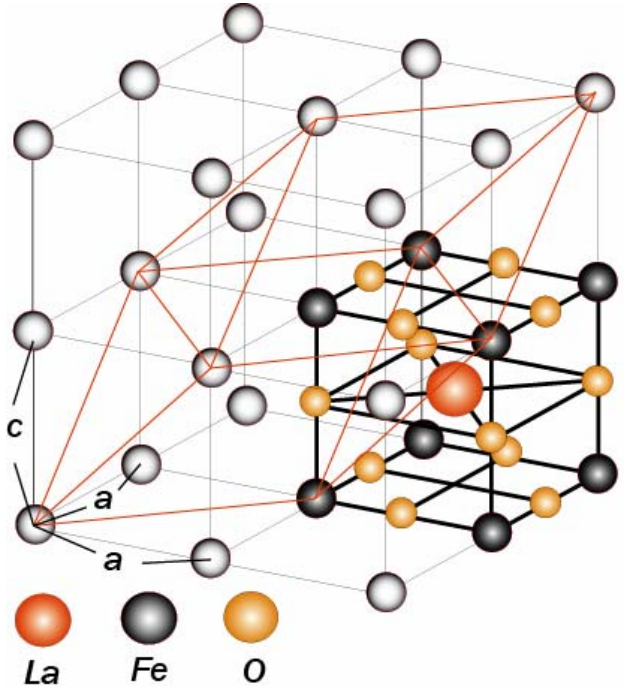

$LaFeO_3$: Rhombohedrally distorted perovskite

Calculated Lattice Constants	
a= 3.7822 Å	c= 3.6493 Å

Cutoff Energy : 500 eV
Exchange-Correlation approximation: LDA
K-POINT spacing: 2X2X2

DEFECT EQUILIBRIA

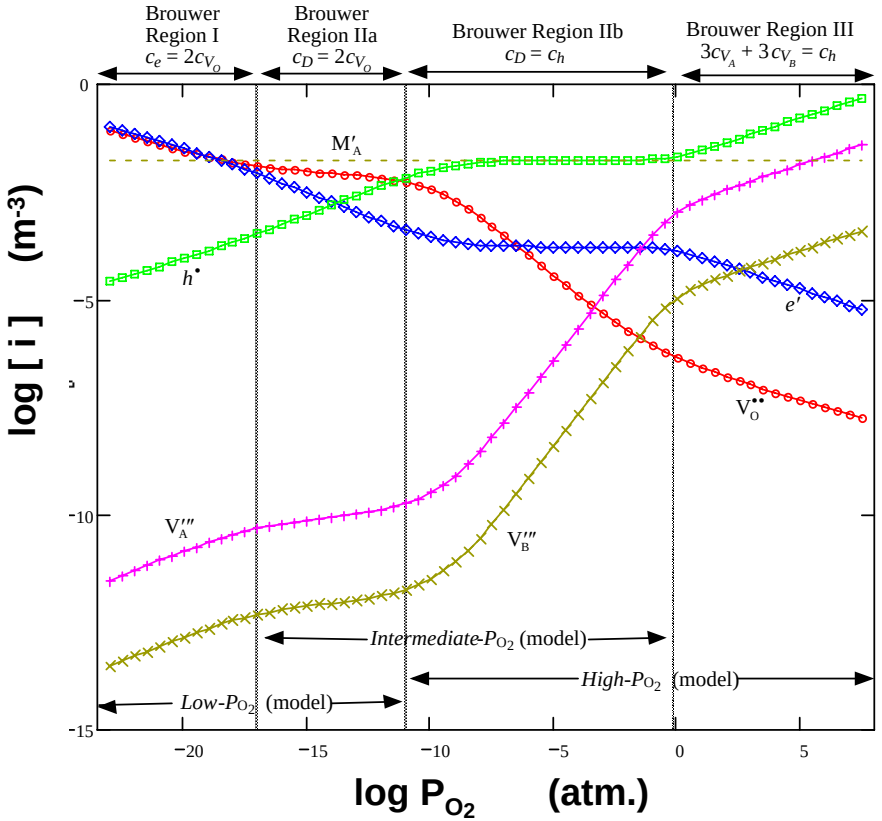

Same approach being applied to perovskites

- Defect equilibria already developed
- Structural optimization in progress

UF-DOE HiTEC

CATHODE DEVELOPMENT

$$O_O^{\times} \leftrightarrow V_O^{\bullet\bullet} + 2e' + \frac{1}{2}O_2$$

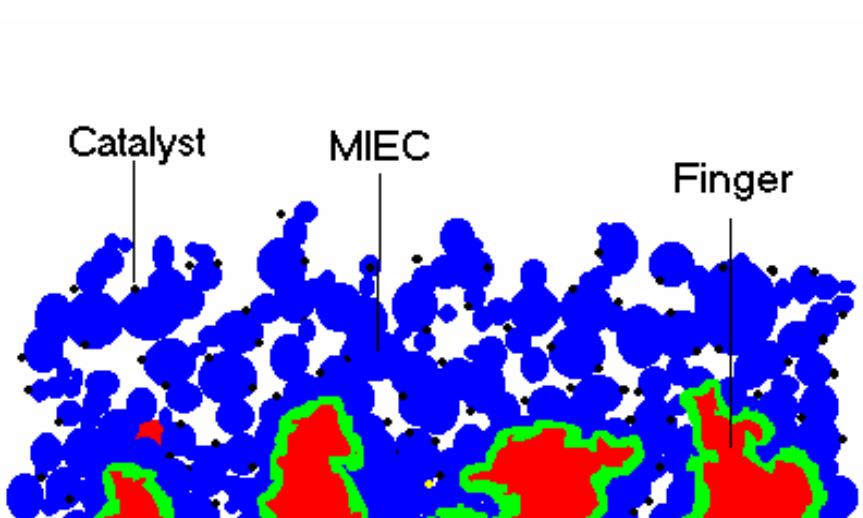

Optimize Microstructure for:

- Activation Polarization
  - Electrocatalytic Activity
    - Increase specific catalytic activity
    - Increase TPB
    - Dispersed catalyst
- Ohmic Polarization
  - Electronic vs. Ionic Transport
    - Electronic conduction path
    - Ionic conduction path
- Concentration Polarization
  - Gas transport
    - Graded porosity
    - Gas vs. solid state transport

CATHODE DEVELOPMENT - Electrocatalytic Activity

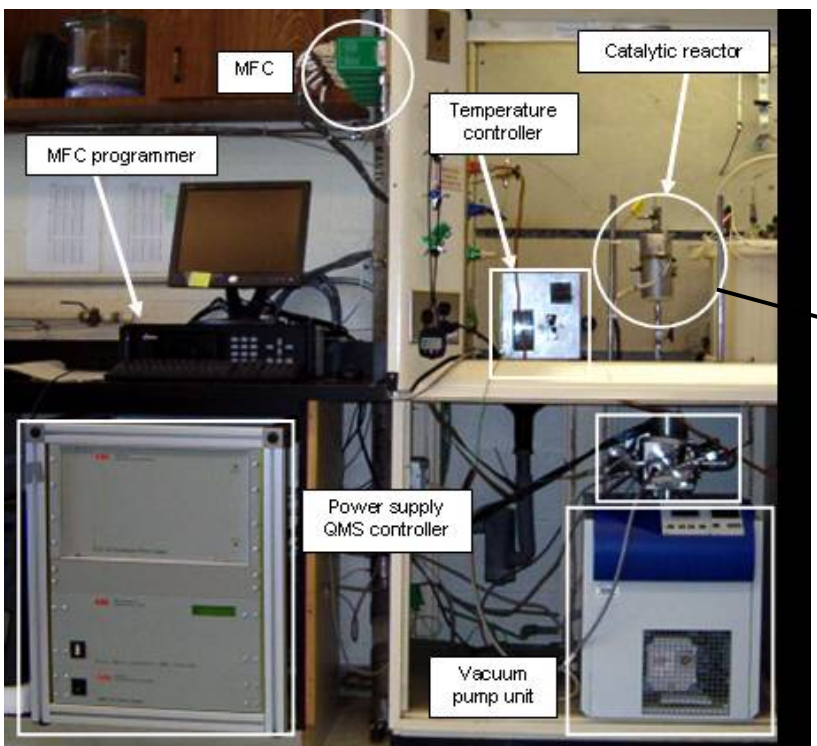

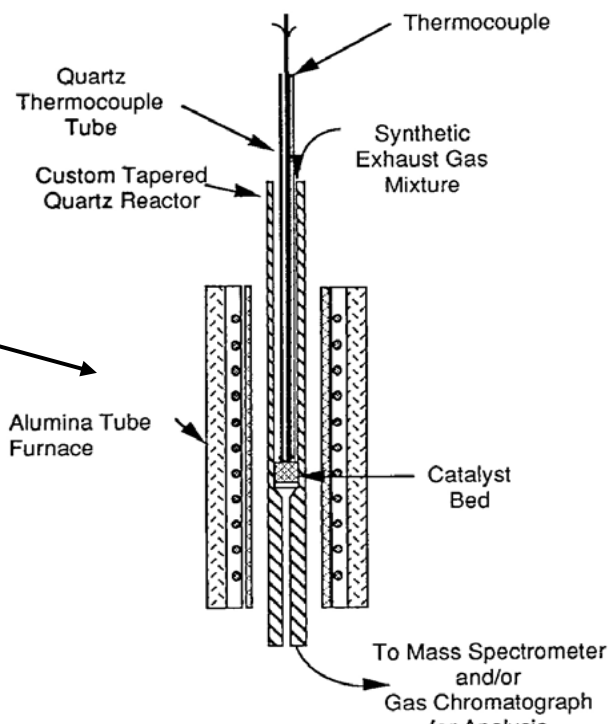

Figure 1. Microreactor

- Temperature programmed reaction (TPR)
  - Ramp temperature in reacting gas mixture to determine catalytic activity and selectivity
- Temperature programmed desorption (TPD)
  - Ramp temperature in He to determine adsorbed species

CATHODE DEVELOPMENT - Electrocatalytic Activity

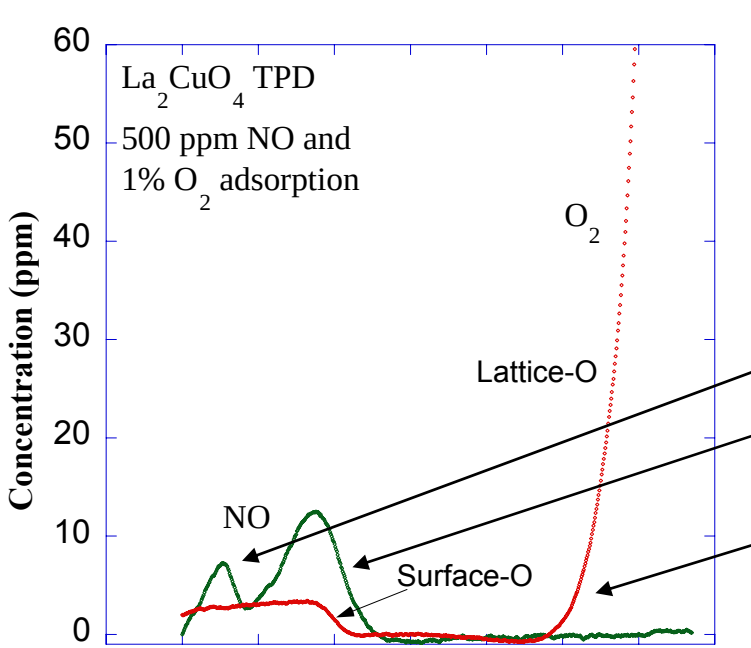

Set up for $^{18}O_2$ probe molecule with ^{16}O oxide catalyst:

$^{18}O_2 = {}^{18}O_2$ - phys-adsorbed

$^{18}O_2 = {}^{18}O^{16}O$ - scrambled product

$^{18}O_2 = {}^{16}O_2$ - lattice oxygen

Kinetics of scrambled product formation indicative of charge transfer reaction and surface exchange coefficient, k_o

NO used as probe molecule:

$NO = 1/2N_2 + 1/2O_2$

vs.

$O_2 = O_2$

CATHODE DEVELOPMENT - Electrocatalytic Activity

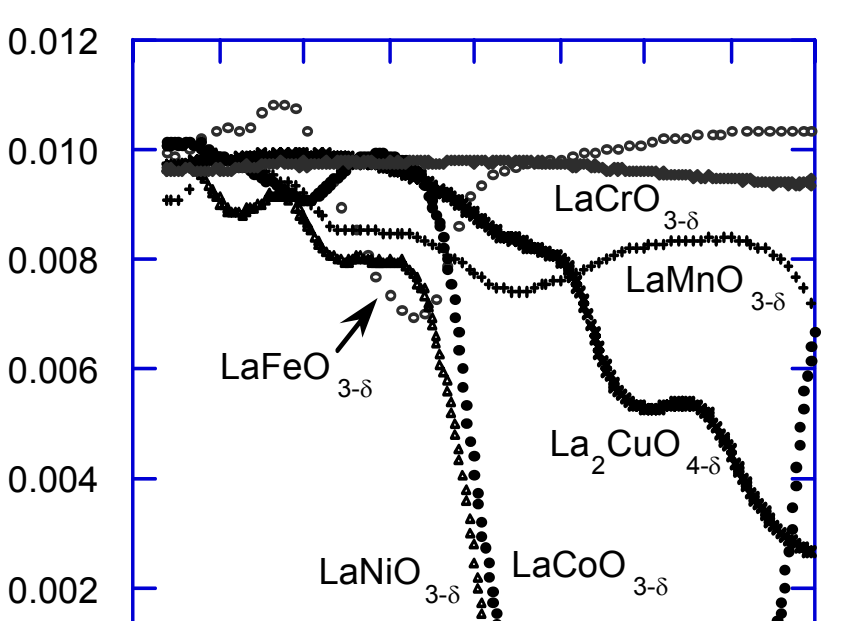

TPR of NO over partially reduced $LaBO_{3-\delta}$

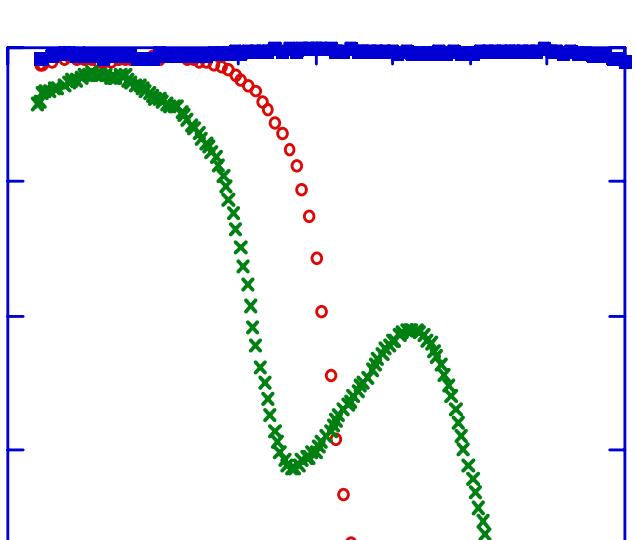

TPR of NO over $La_{1-x}Sr_xCo_{1-y}(Ru/Fe)_yO_{3-\delta}$

Effect of B-site transition metal on catalytic activity:

- Cations with partially filled d-orbitals (Co, Ni) more active
- Ru most active

CATHODE DEVELOPMENT - Electrocatalytic Activity

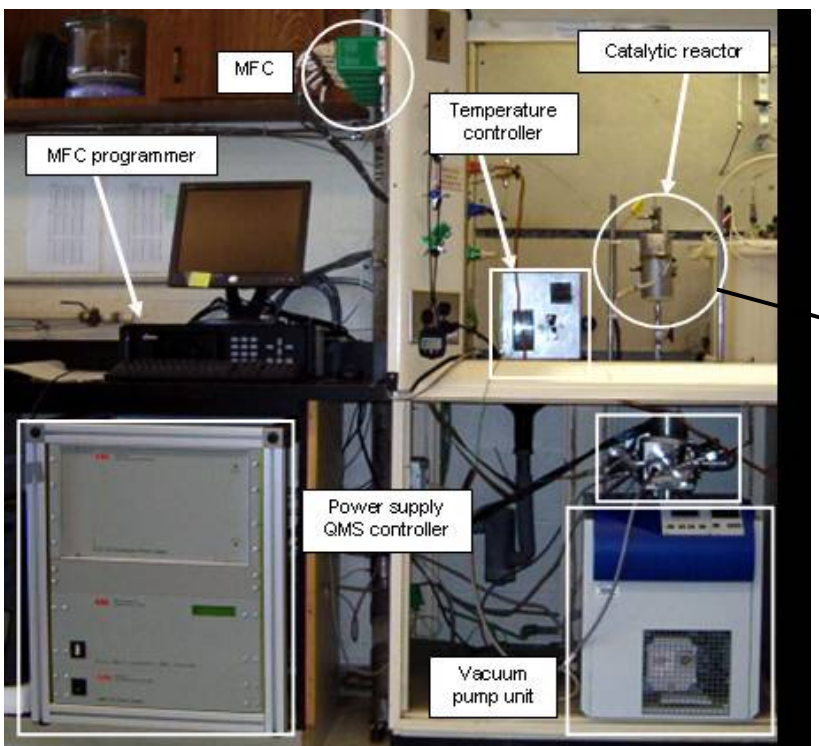

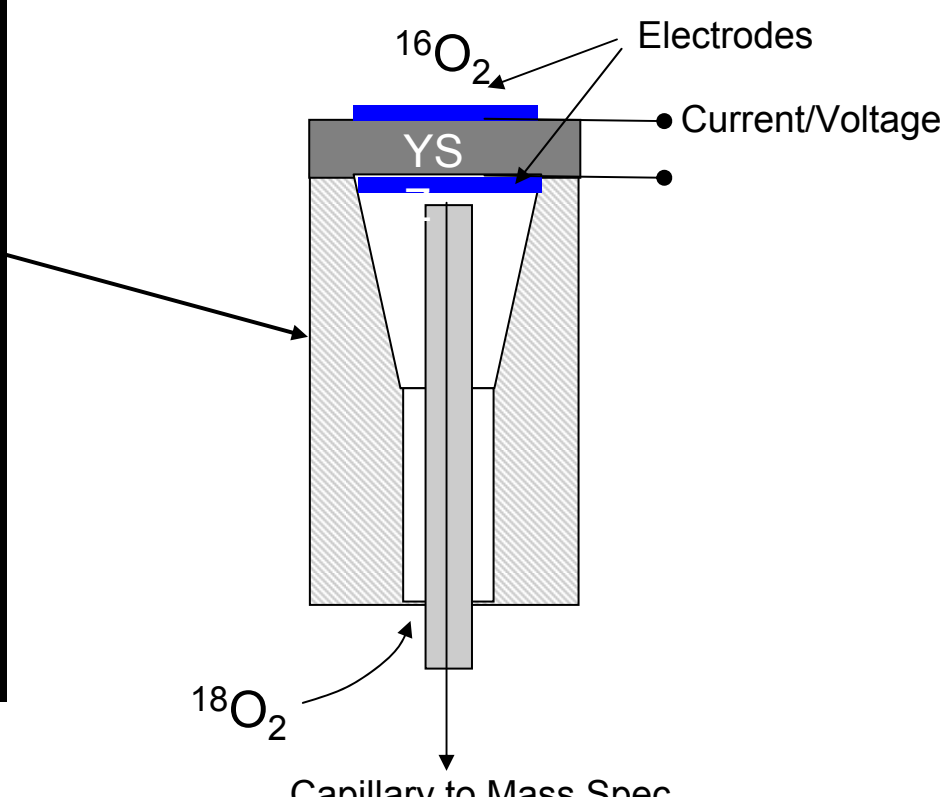

- Potential programmed reaction (PPR)
  - Ramp voltage in reacting gas mixture to determine catalytic activity and selectivity
- Potential programmed desorption (PPD)
  - Ramp voltage in He to determine adsorbed species

CATHODE DEVELOPMENT - Electrocatalytic Activity

$$O_O^{\times} \leftrightarrow V_O^{\bullet\bullet} + 2e' + \frac{1}{2}O_2$$

$$K_R = \overrightarrow{k_o}/\overleftarrow{k_o}$$

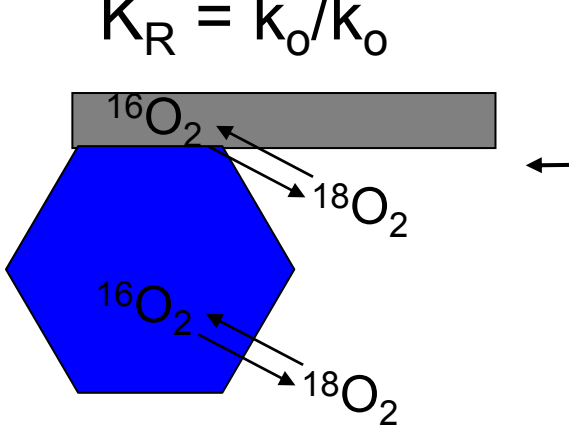

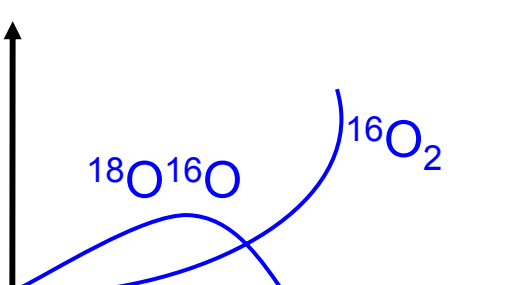

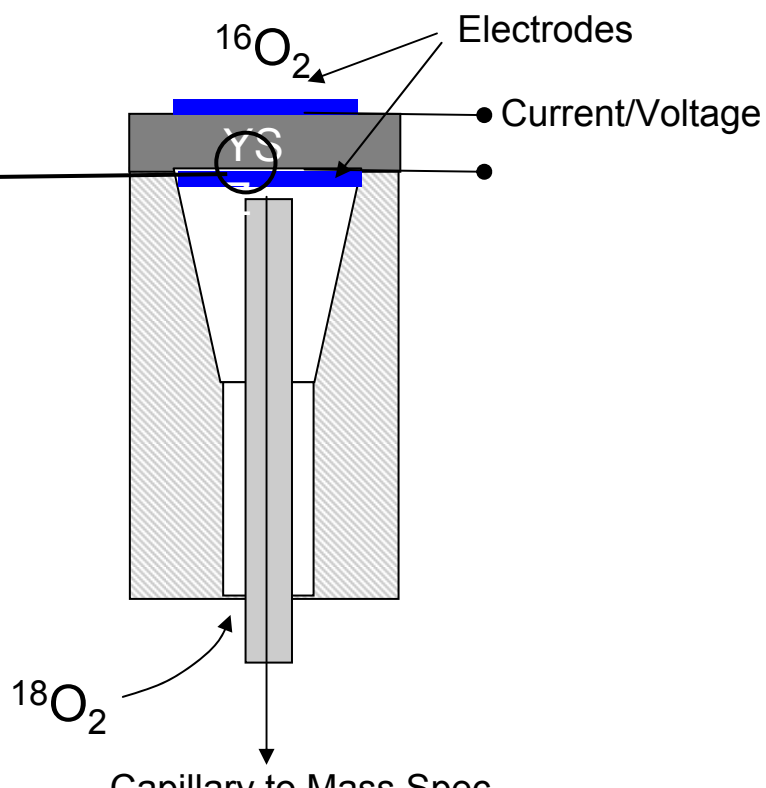

Include:

- Electrode structure
- Current-voltage behavior: $i_o \sim k_o$, $k = f(V)$

CATHODE DEVELOPMENT - Electronic vs. Ionic Transport

Benchmark

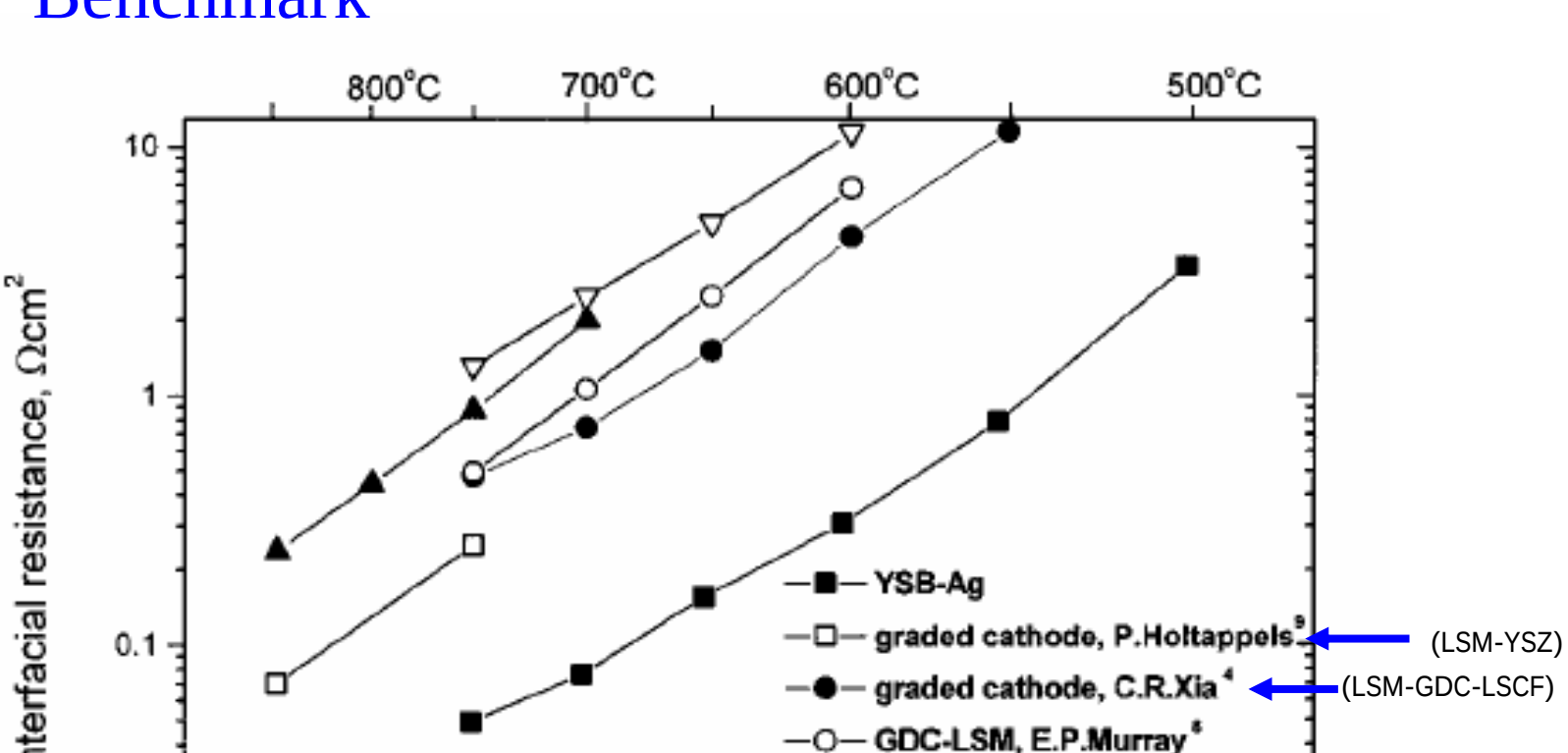

C. Xia, Y. Zhang, M. Liu, Appl. Phys. Lett., Vol. 82, No. 6, 10 February 2003

CATHODE DEVELOPMENT - Electronic vs. Ionic Transport

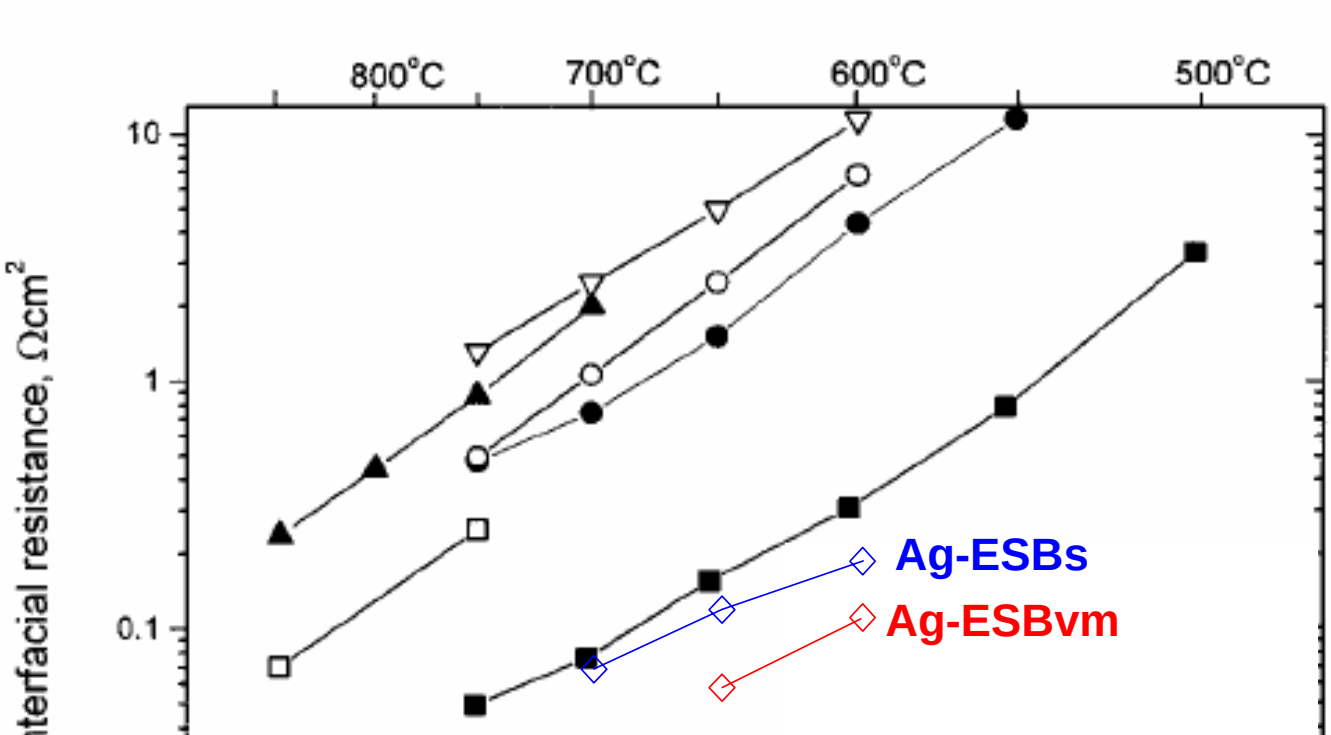

C. Xia, Y. Zhang, M. Liu, Appl. Phys. Lett., Vol. 82, No. 6, 10 February 2003

CATHODE DEVELOPMENT - Electronic vs. Ionic Transport

Relative size of ionic/electronic conducting phase

- Same volume fractions
- ESB particle size reduction

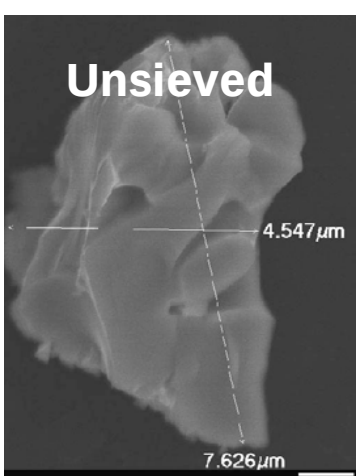

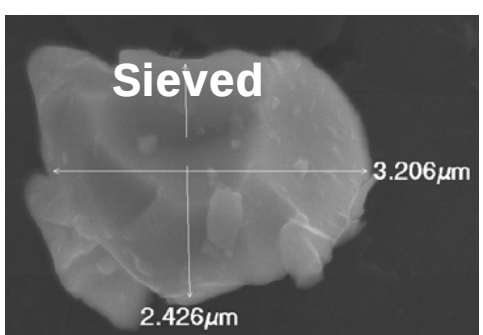

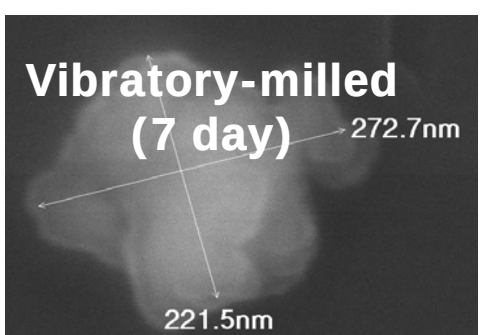

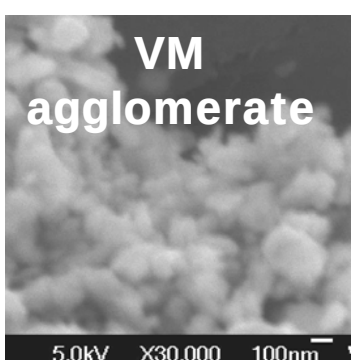

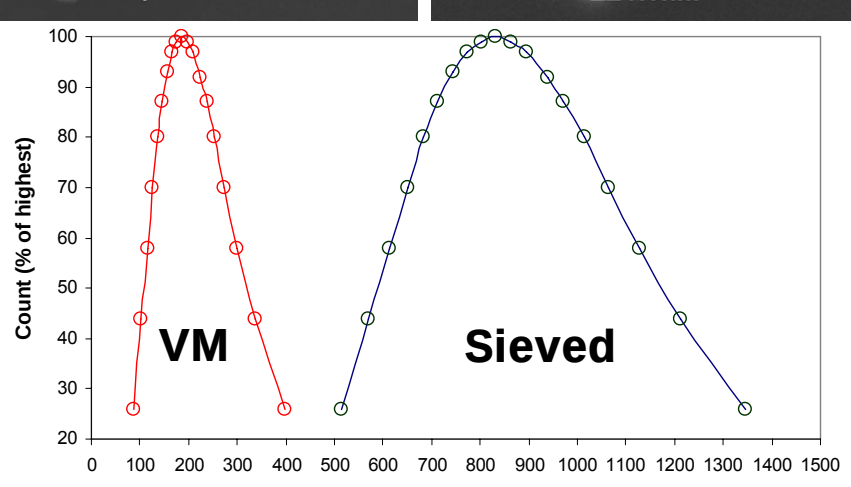

CATHODE DEVELOPMENT - Electronic vs. Ionic Transport

Stability @ 650˚C (100h) in air

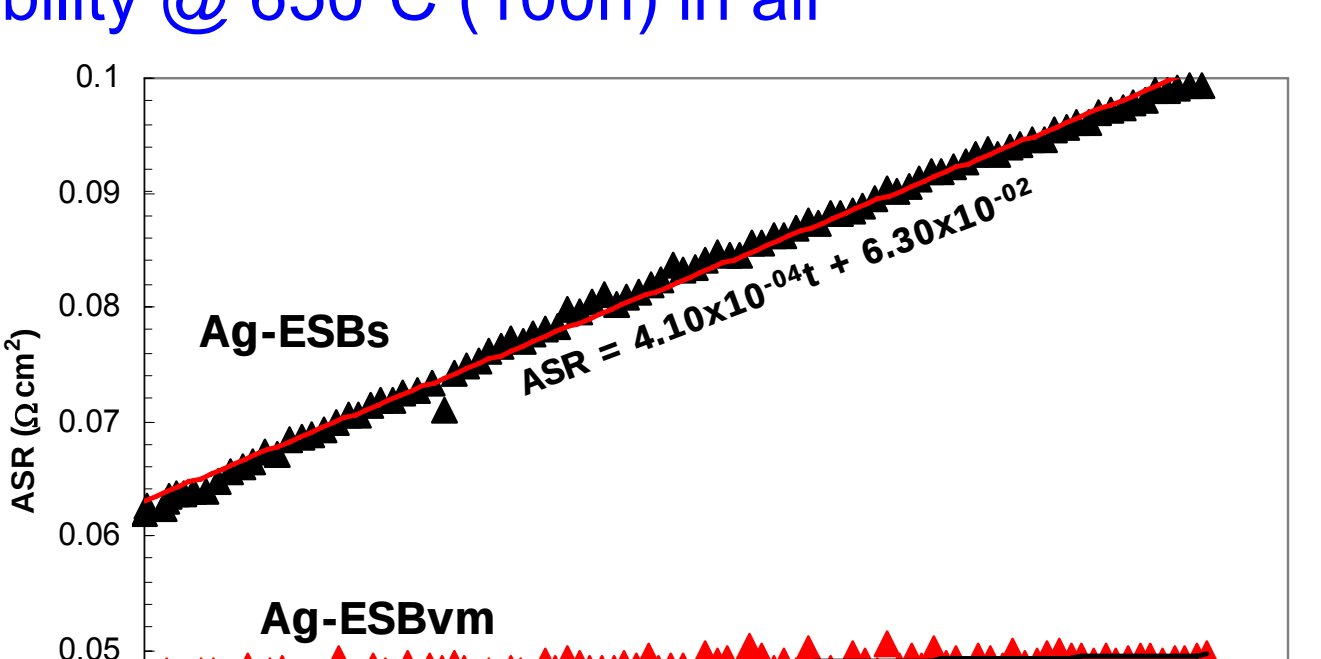

Smaller ESB particle size increases stability

However, ASR still increases with time under current due to electromigration of Ag

New Cathode Materials - Pyrochlores

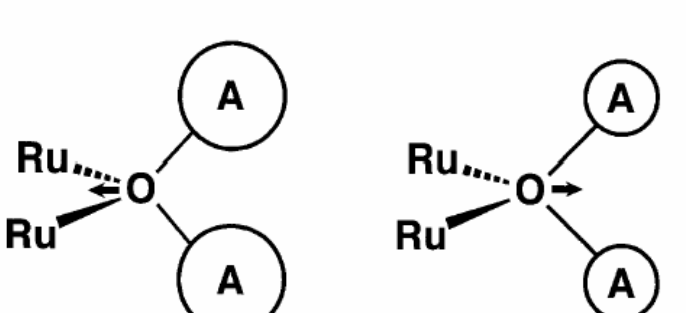

T, °C

QuickTime™ and a
TIFF (Uncompressed) decompressor
are needed to see this picture.

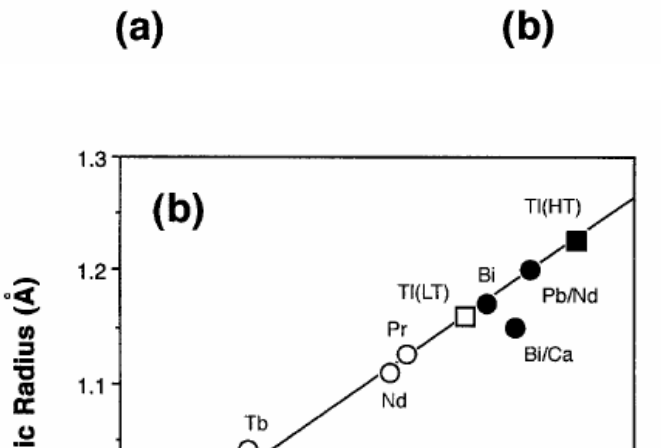

- High Electrical Conductivity ~10^3 Scm^{-1}
- Metallic (increases with decreasing temperature)

K. S.*Lee, J. Solid state Chem.* ***131*** *(1997), 405*

CATHODE DEVELOPMENT - Electronic vs. Ionic Transport

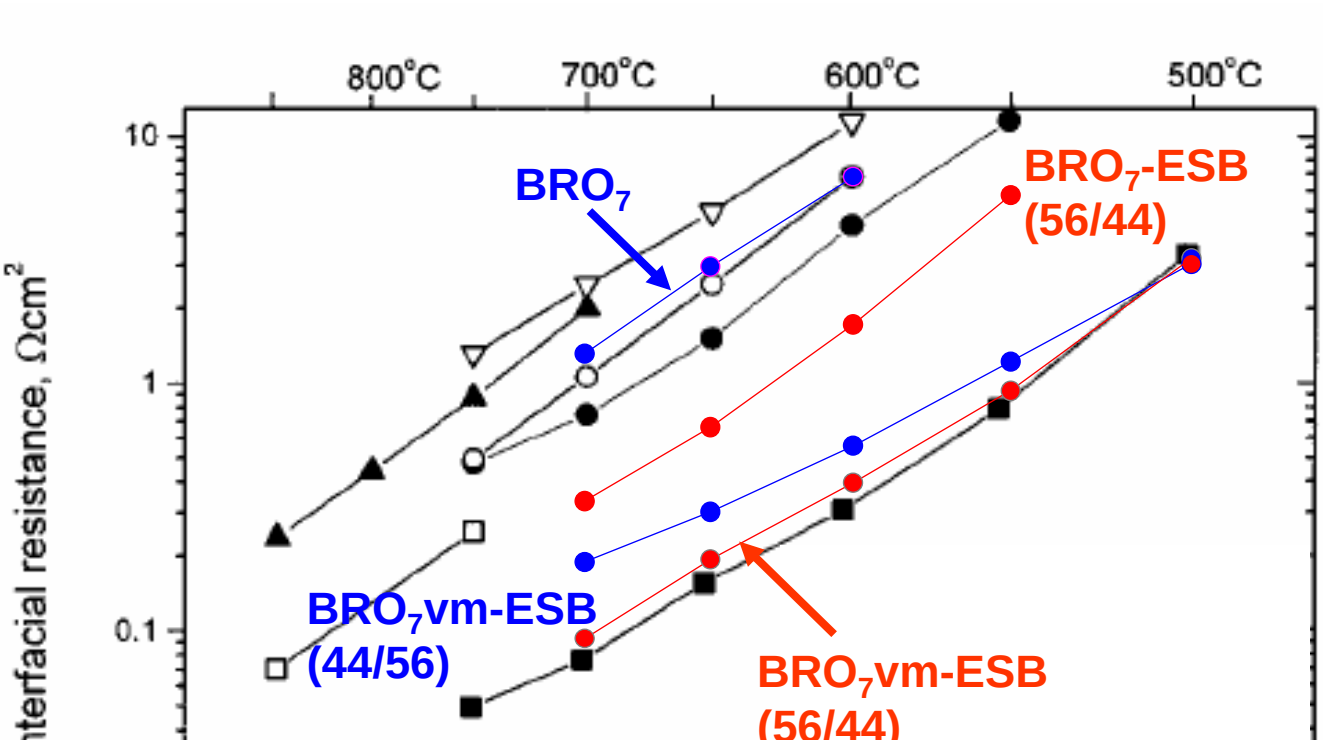

C. Xia, Y. Zhang, M. Liu, Appl. Phys. Lett., Vol. 82, No. 6, 10 February 2003

CATHODE DEVELOPMENT - Electronic vs. Ionic Transport

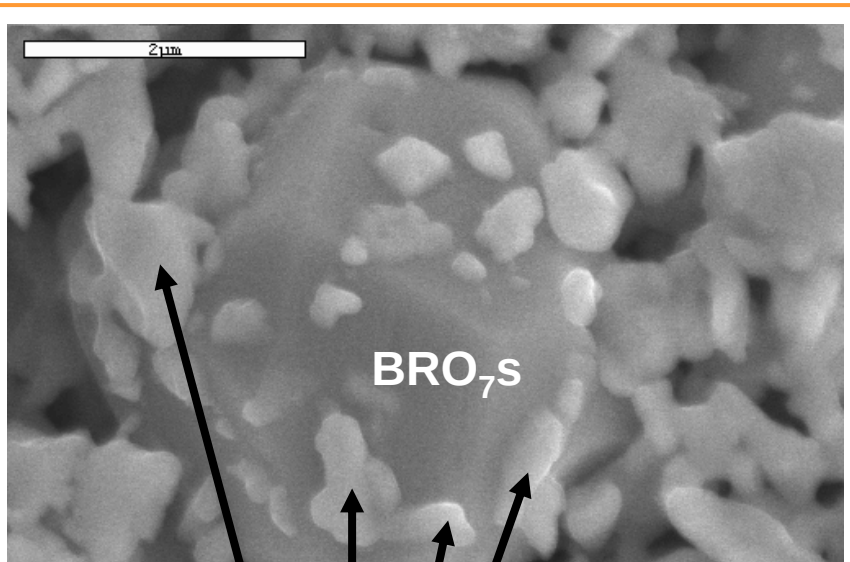

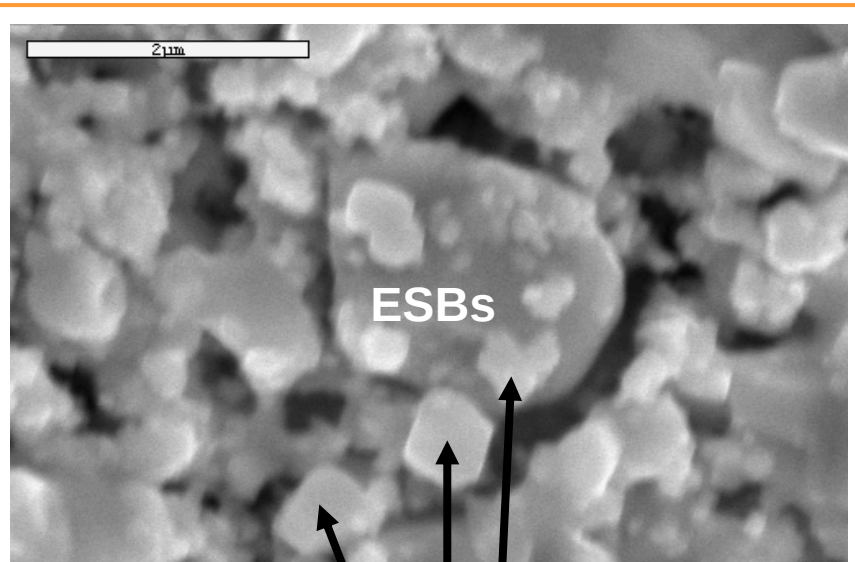

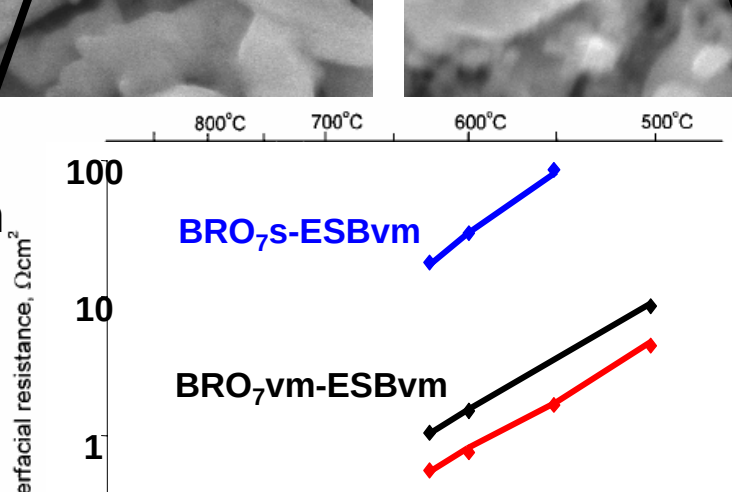

EXTEND MODEL TO INCLUDE MICROSTRUCTURAL EFFECTS

CATHODE

$$P_{O_2,\text{cathode-electrolyte interface}} = P_{\text{atmos}} - \left(P_{\text{atmos}} - P_{O_2@\text{air}}\right)\exp\left(\frac{kT}{4q}\cdot\frac{\tau_c}{D_c}\cdot\frac{L_c}{\varepsilon_c}\cdot J\right)$$

tortuosity

gas diffusivity

porosity

ANODE

$$P_{H_2,\text{anode-electrolyte interface}} = P_{H_2@\text{fuel}} - \frac{kT}{2q}\cdot\frac{\tau_a}{D_a}\cdot\frac{L_a}{\varepsilon_a}\cdot J$$

$$P_{H_2O,\text{anode-electrolyte interface}} = P_{H_2O@\text{fuel}} + \frac{kT}{2q}\cdot\frac{\tau_a}{D_a}\cdot\frac{L_a}{\varepsilon_a}\cdot J$$

J.-W. Kim, A. Virkar, K.-Z. Fung, K. Mehta and S. Singhal, *J. Electrochem. Soc.*, **146** (1999) 69-78

S. Chan, K. Khor, Z. Xia, *J. Power Sources*, **93** (2001) 130

DEFECT CONCENTRATION

$$K\big|_{J=0}\exp\left(\frac{q\eta}{kT}\right) = \frac{c_V c_e^2}{1-c_V}P_{O_2}^{\frac{1}{2}}$$

ACTIVATION OVERPOTENTIAL

$$J = J_0\left[\exp\left(\frac{q}{kT}\alpha\eta\right) - \exp\left(-\frac{q}{kT}(1-\alpha)\eta\right)\right]$$

POTENTIAL

$$\Phi_{ext} - \Phi_{th} - \frac{k_B T}{z_V q}\ln\frac{c_{V_L}}{c_{V_0}} = \frac{z_V u_e + u_V\left(1-\dfrac{\eta}{\Phi_{th}-\Phi_{ext}}\right)}{u_e - u_V\left(1-\dfrac{\eta}{\Phi_{th}-\Phi_{ext}}\right)}\cdot\frac{k_B T}{z_V q}\ln\frac{c_{V_L} - \dfrac{u_e c_A / z_V}{u_e - u_V\left(1-\dfrac{\eta}{\Phi_{th}-\Phi_{ext}}\right)}}{c_{V_0} - \dfrac{u_e c_A / z_V}{u_e - u_V\left(1-\dfrac{\eta}{\Phi_{th}-\Phi_{ext}}\right)}}$$

EXTEND MODEL TO INCLUDE MICROSTRUCTURAL EFFECTS

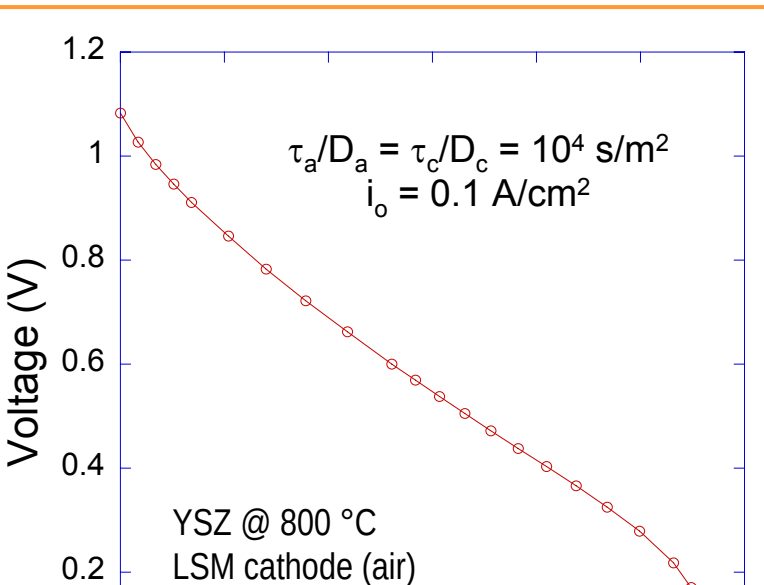

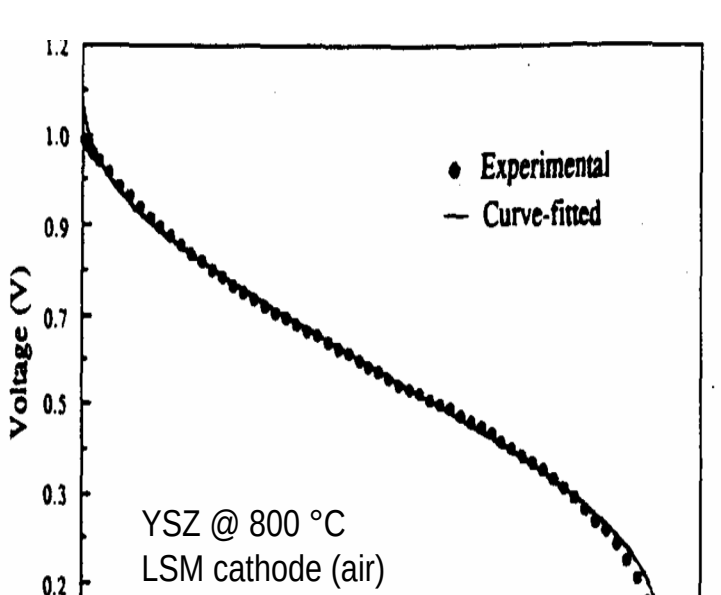

Figure 5. Experimental data at 800°C and the corresponding best fit to Eq. 45.

- Electrochemical model (with pore diffusion incorporated) matches "Virkar"* model, but with less fitting parameters, (3 vs. 10)
- Fitting parameters: τ_a/D_a (effective tortuosity anode), τ_c/D_c (effective tortuosity cathode) and i_o (exchange current density).

*J.-W. Kim, A. Virkar, K.-Z. Fung, K. Mehta and S. Singhal, *J. Electrochem. Soc.*, **146** (1999) 69-78

EXTEND MODEL TO INCLUDE MICROSTRUCTURAL EFFECTS

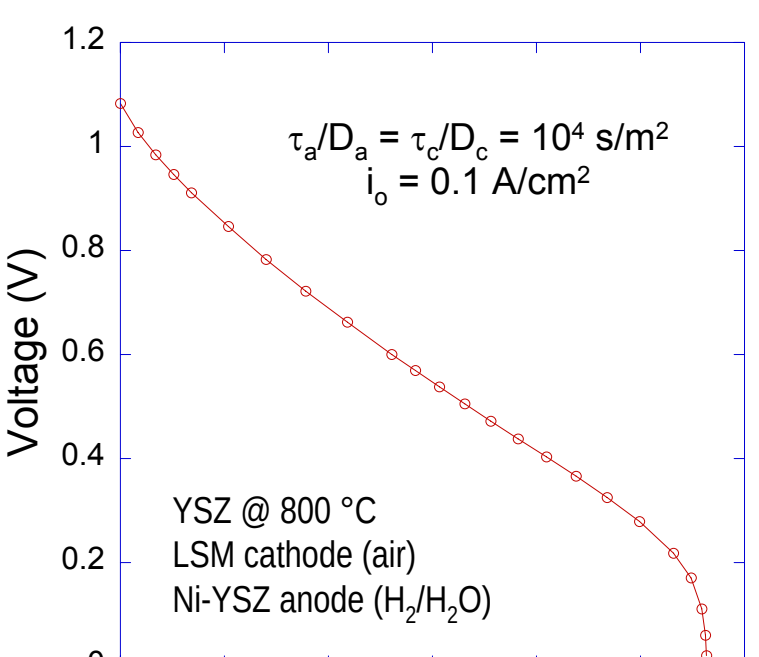

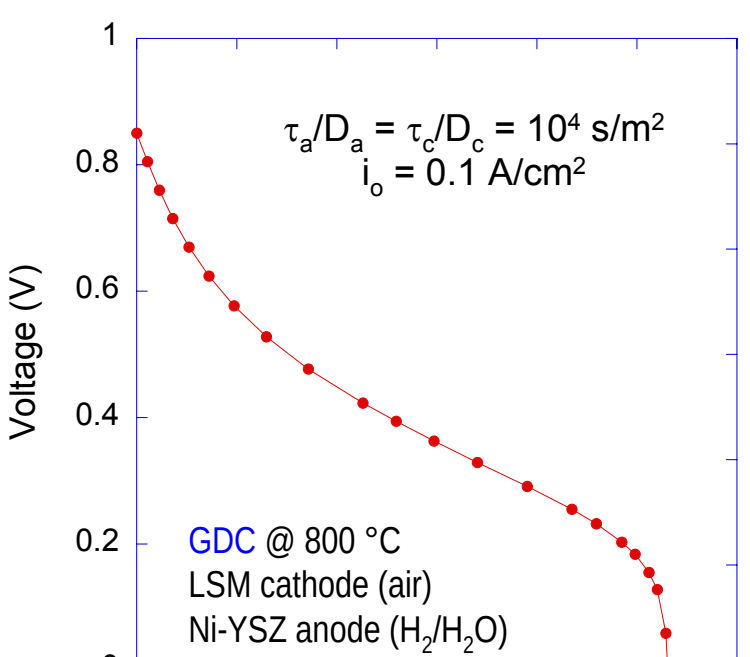

I-V & power density curves can also be generated for mixed conducting materials:

- Electrolytes such as GDC (above)
  - -Shows reduction in OCP and current density due to low t_i at 800°C
- Cathodes such as LSF and LSCF (near future)

EXTEND MODEL TO INCLUDE MICROSTRUCTURAL EFFECTS

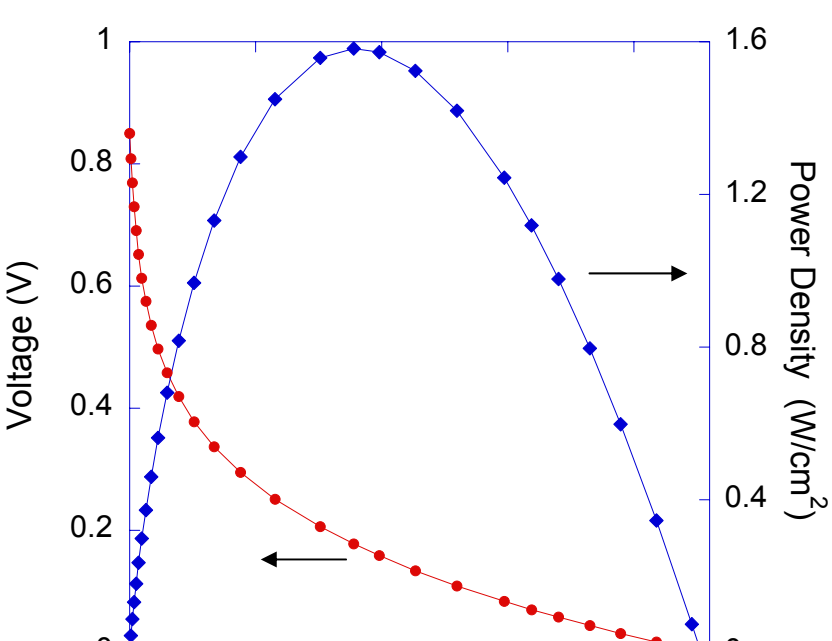

$\tau_a/D_a = \tau_c/D_c = 10^2$ s/m^2
$i_o = 0.1$ A/cm^2

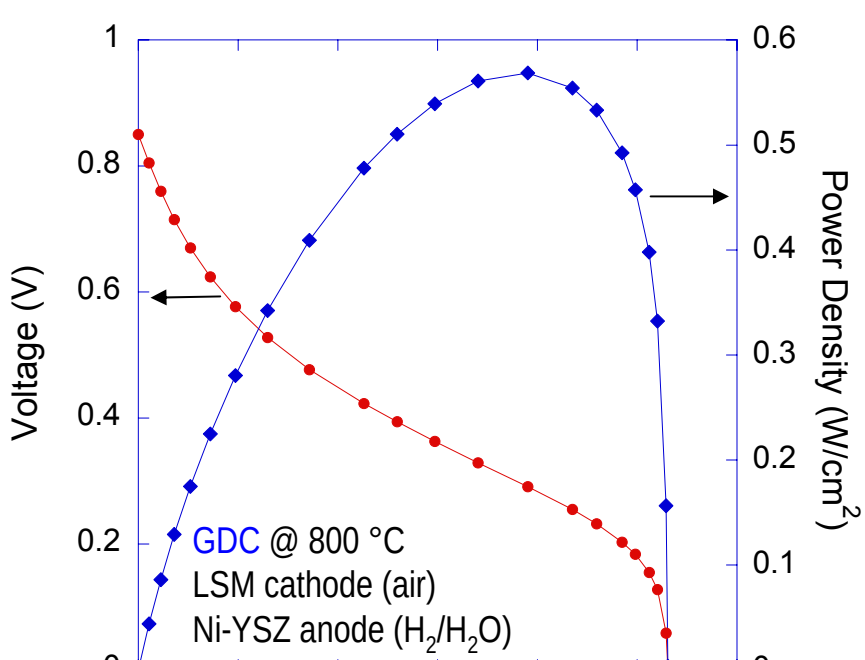

$\tau_a/D_a = \tau_c/D_c = 10^4$ s/m^2
$i_o = 0.1$ A/cm^2

Model shows decrease in effective tortuosity (τ/D) can dramatically increases power density

DECONVOLUTION OF CATHODE MECHANISM

Oxygen exchange at TPB (0.0001 s)

Ionic conductivity through electrolyte grain boundary

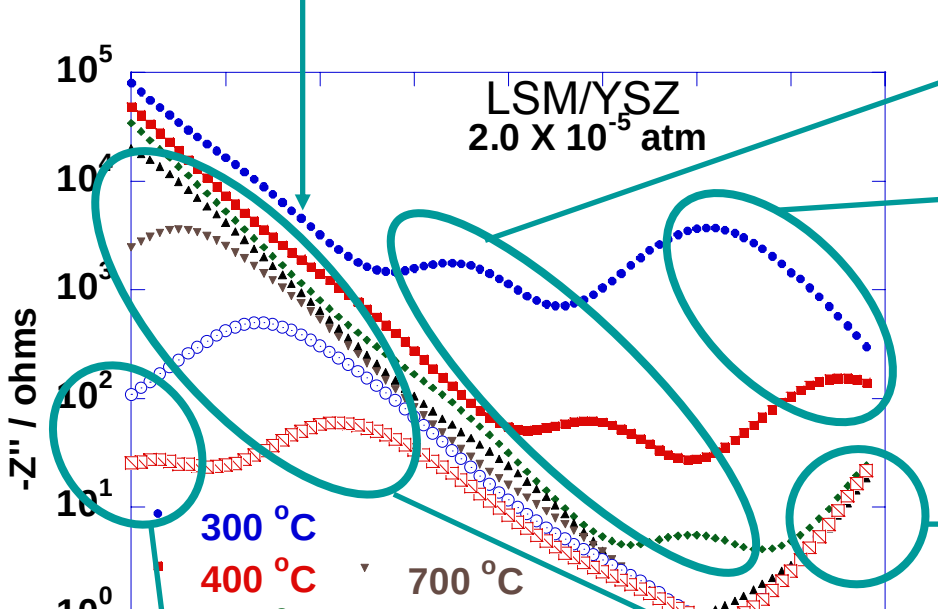

Ionic conductivity in the bulk electrolyte

Artifacts minimized by nulling

Dissociation and surface diffusion of O-species on LSM to TPB (0.18 s)

Oxygen diffusion through through porous cathode (5.9 s)

DECONVOLUTION OF CATHODE MECHANISM

Step #	Process identity	"x" in $R \propto pO_2^x$	E_a (eV)	τ (s) at 800 °C
1	Ionic diffusion through electrolyte bulk.	~0 Independent	1.10 1.05[d]	-
2	Ionic diffusion across electrolyte grain boundary.	~0 Independent	1.04 1.16[d]	-
3	Migration and incorporation of O^{2-} from TPB into YSZ.	~0 Independent[a]	0.97 1.10[a] 1.13[b]	8.5×10^{-5} 1.6×10^{-5}[a]
4	Dissociation and surface diffusion of O-species on LSM.	-0.15 -0.268[a,c]	1.2 1.61[a] 1.69[b]	0.18 0.016[a]
5	Gas diffusion through porous electrode.	-1.1 -1.02[a,c]	~0 ~0[a]	5.9 0.16[a]

a) X. J. Chen et al. / Journal of Power Sources 123 (2003) 17
b) Jiang et al. / J. of Electrochemical Society 147 (2000) 3195
c) Kim et al. / Solid State Ionics, 143 (2001) 379
d) Guo, Maier / J. of Electrochemical Society 148 (2001) E121

DECONVOLUTION OF CATHODE MECHANISM

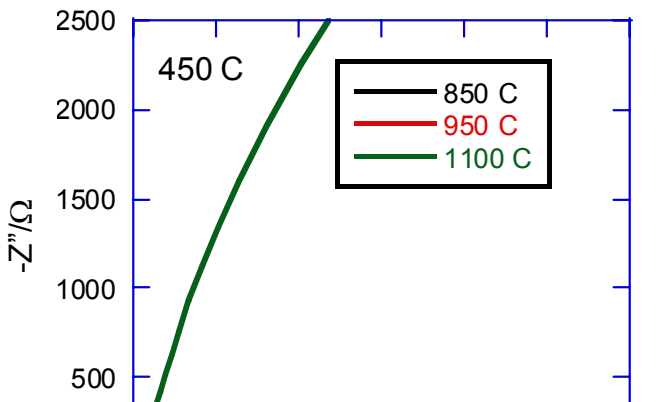

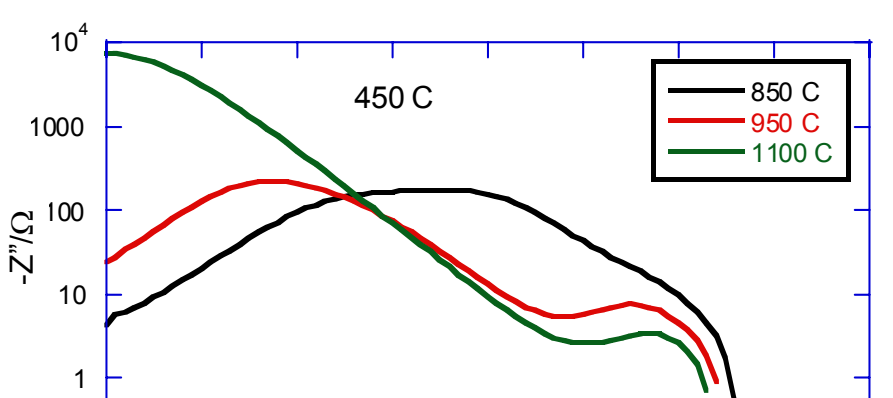

Microstructure/Impedance - LSCF Sintering Temperature Effect

850 °C

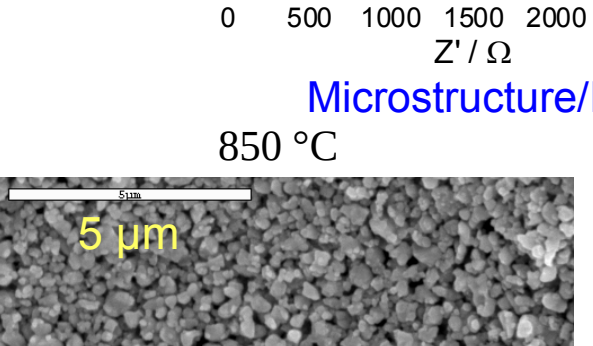

950 °C

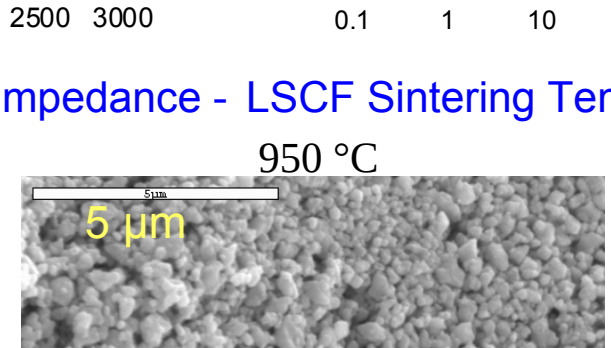

1100 °C

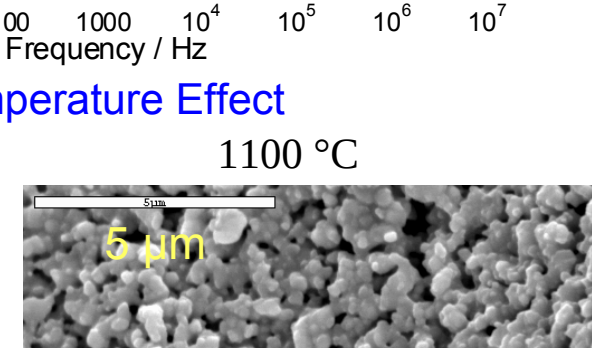

Highest temperature coarsens microstructure - multiple changes to impedance

Powder supplied by NexTech

QUANTIFYING MICROSTRUCTURE

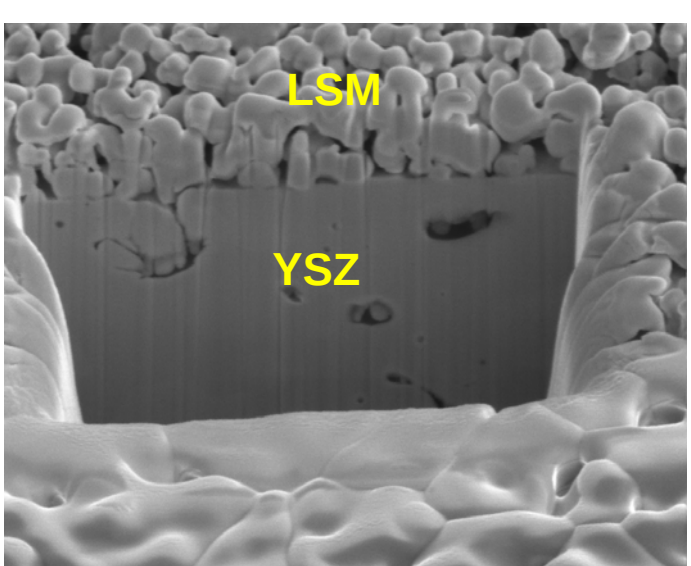

Focused Ion Beam

- Enables 3-D analysis of electrode microstructure
  - Particle-size, pore-size, & distribution
  - Triple-phase boundary density
  - Tortuosity

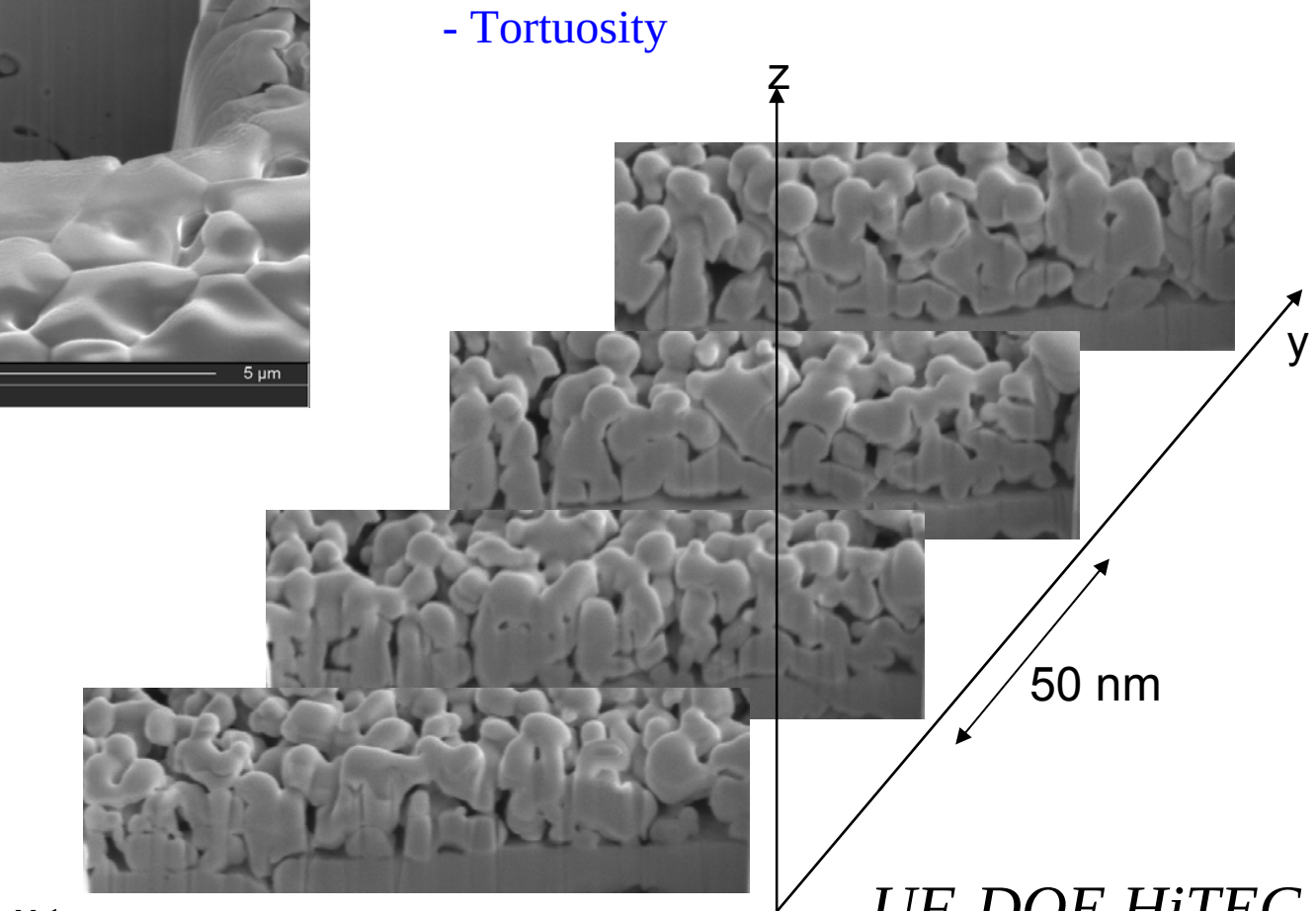

QUANTIFYING MICROSTRUCTURE

AREA FRACTION

- Measure grain to interface line distance
- LSM-YSZ Grain Interface
- Pore-YSZ Interface

- Sample shown is screen-printed LSM sintered at 1350° C

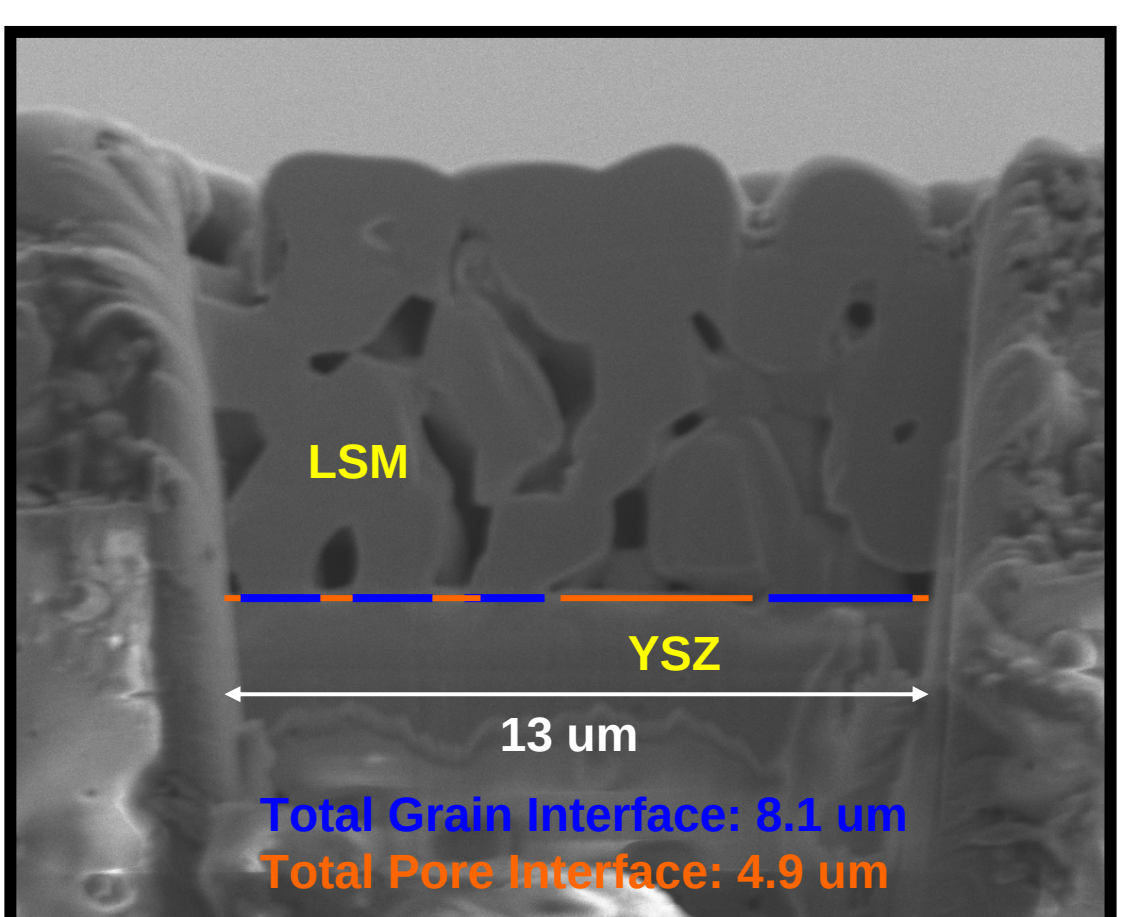

QUANTIFYING MICROSTRUCTURE

AREA FRACTION

By combining consecutive line analysis, area density analysis is achieved.

Percent of grain density per total area is current approach.

Example: 67% grain-to-interface density

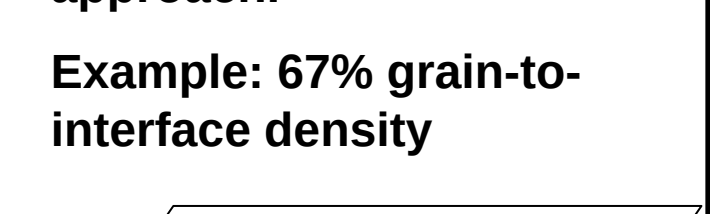

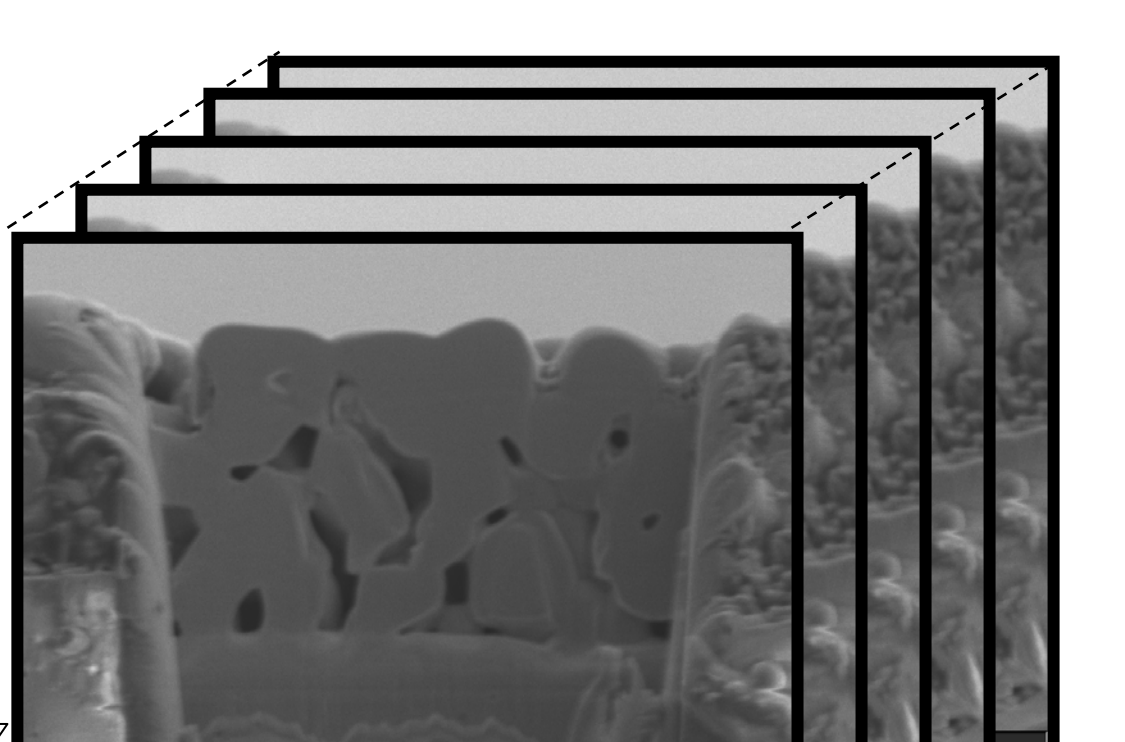

QUANTIFYING MICROSTRUCTURE

VOLUME FRACTION

- Measure grain and pore area
- By analyzing over multiple evenly spaced slices, volume fraction can be determined.
- Ex.: 89% Area Grain
- Sample shown is screen-printed LSM sintered at 1350˚ C

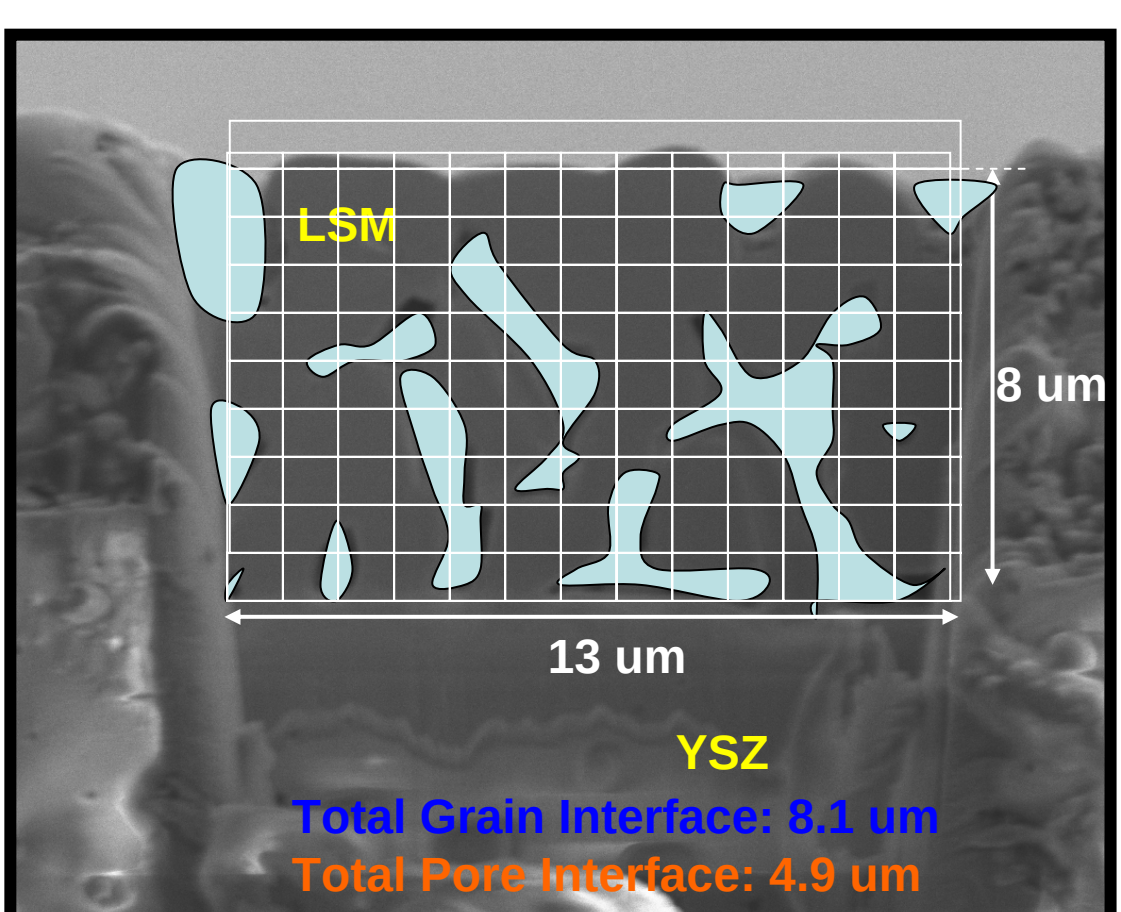

QUANTIFYING MICROSTRUCTURE

VOLUME FRACTION

By combining consecutive area analysis, a volume density analysis can be achieved.

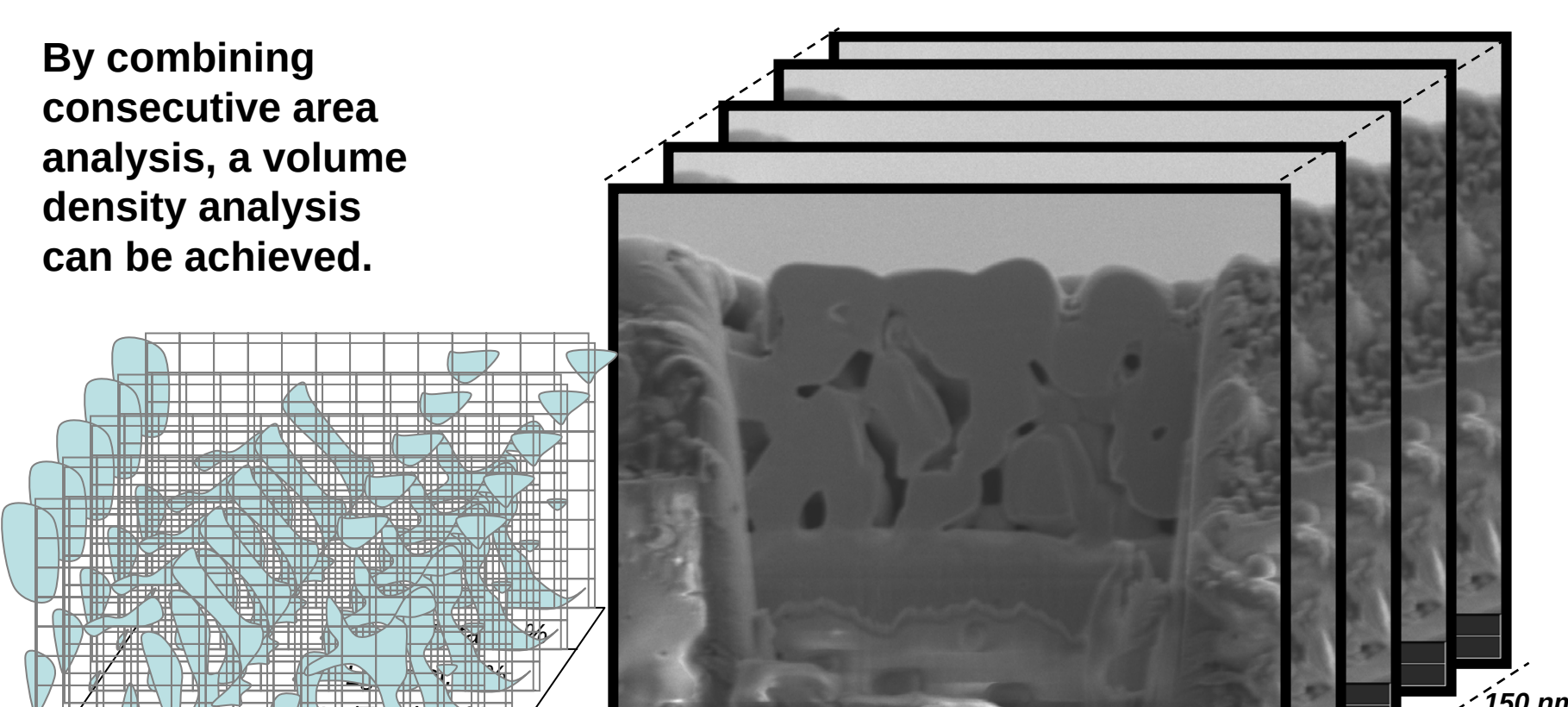

QUANTIFYING MICROSTRUCTURE

TRIPLE PHASE LINE DENSITY

- Calculate triple phase boundary density
- **Triple-phase points**

- Sample shown is screen-printed LSM sintered at 1350˚ C

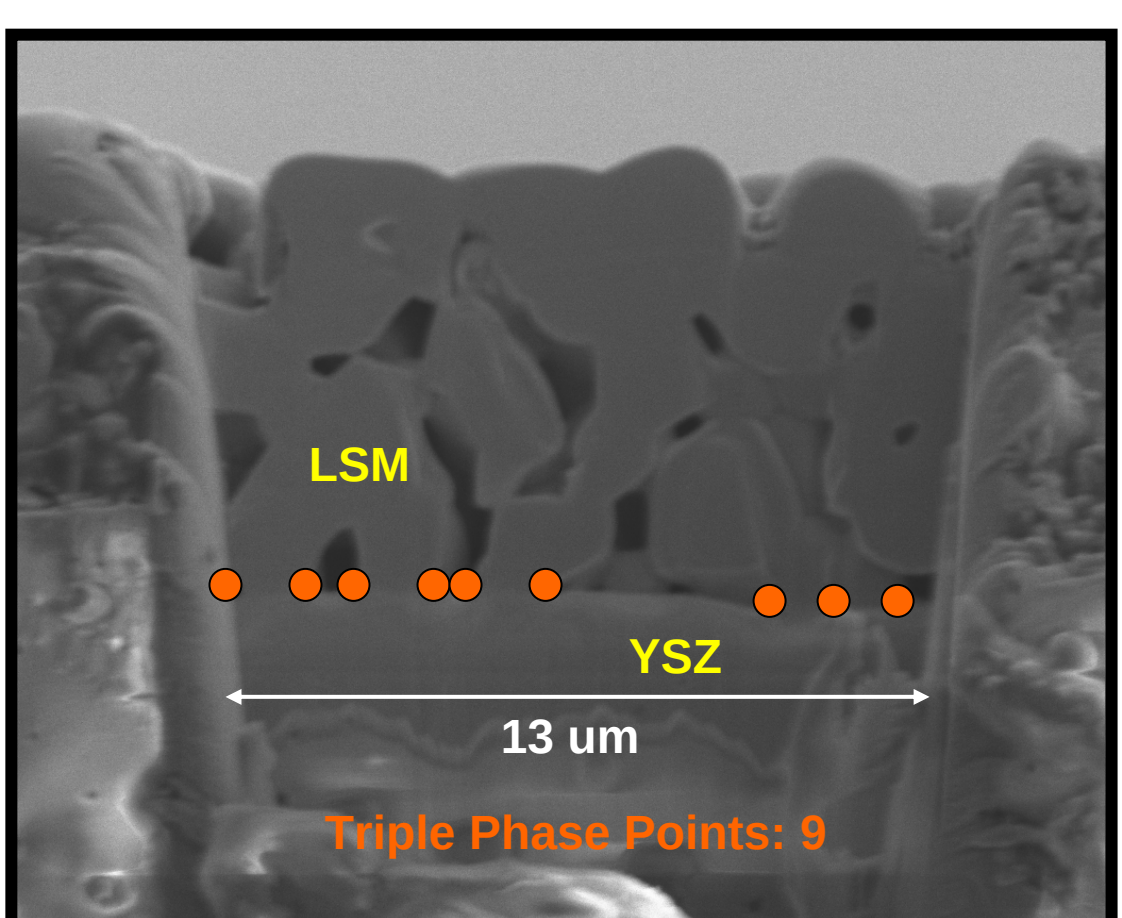

QUANTIFYING MICROSTRUCTURE

TRIPLE PHASE LINE DENSITY

By connecting all of the triple phase points, the interface lines can be determined in the sample.

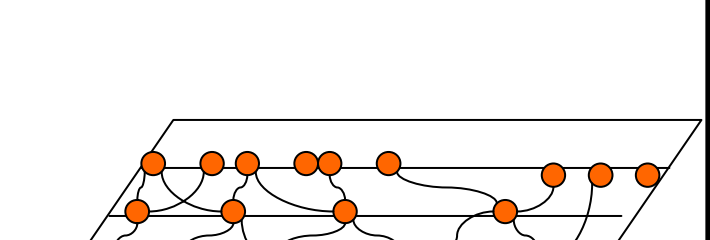

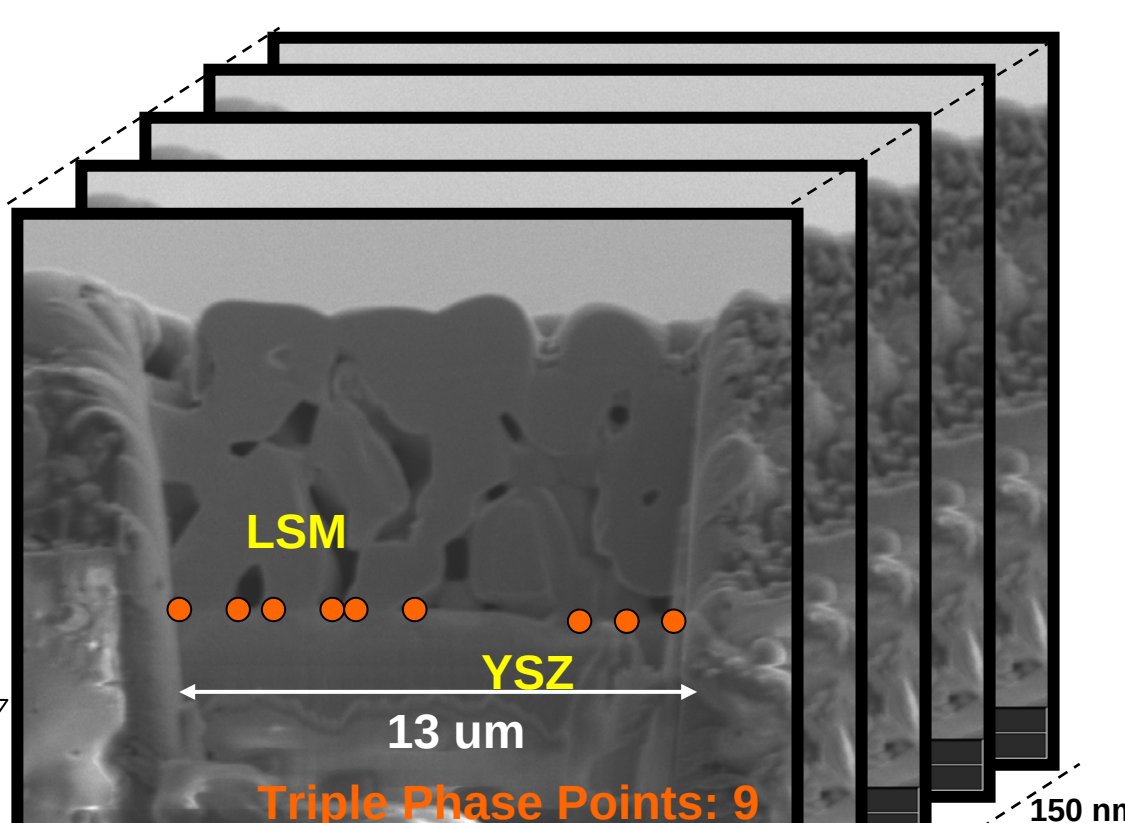

QUANTIFYING MICROSTRUCTURE

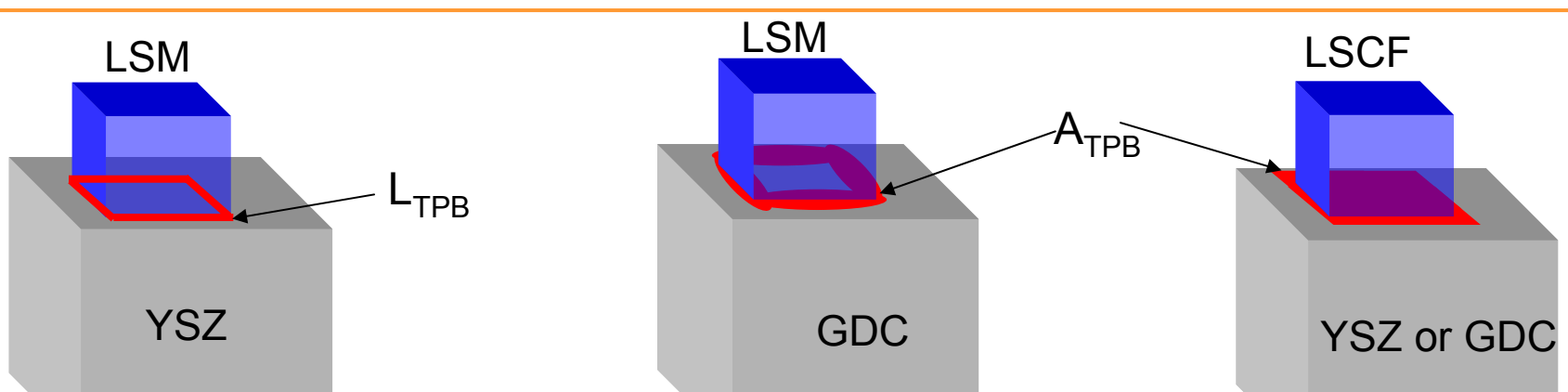

Butler-Volmer Equation: $J = J_0[\exp(q\alpha\eta_{act}/kT) - \exp(-q(1-\alpha)\eta_{act}/kT)]$

$J_0 = j_0 \times A_{TPB} = L_{TPB} \times w_{TPB}$

LSM/YSZ $w_{TPB} \approx$ Debye length

LSM/GDC, LSCF/YSZ, LSCF/GDC $w_{TPB} >$ Debye length

$w_{TPB} \equiv f$(geometry, contact area, material property)

QUANTIFYING MICROSTRUCTURE

Tortuosity

$\tau = z_{path}/z_{thickness}$

QuickTime™ and a
decompressor
are needed to see this picture.

LSM (Nextech) on YSZ

Consecutive 50nm slices

ACKNOWLEDGEMENT

Collaborating Faculty:
Dr. Kevin Jones - FIB/SEM Characterization
Dr.'s Susan Sinnott & Simon Philpott - Computational Materials
Dr. Fereshteh Ebrahimi - Mechanical Properties
Dr. Juan Nino - Novel Oxide Materials Development
Dr. Wolfgang Sigmund - Novel Synthesis & Microstructures
Dr. Hans Seifert - Materials Thermodynamics
Dr. Xin Guo - Nano Ionics and Interfaces

Results by post-docs:
Dr. Keith Duncan, Dr. Jiho Yoo & Dr. Heesung Yoon
Results by graduated students:
Dr. Abhishek Jaiswall, Dr. Jun-Young Park, Dr. Jamie Rhodes, Dr. Sun-Ju Song, Dr. Keith Duncan, Terry Clites, Su-Ho Jung, Sai Boyapati, Naixiong Jiang
Results by current graduate students:
Jeremiah Smith, Matthew Camaratta, Sean Bishop, Yanli Wang, Briggs White, Joshua Taylor, Vincenzo Esposito, Chiara Abate, Jin Soo Ahn, Aidhy Dilpuneet, Brian Blackburn, Chin-Tang Hu, Shobit Omar, Eric Armstrong, Martin VanAssche, Cynthia Chao, Eric Macam, Tak-keun Oh, Doh Won Jung, Dan Gostovic, Aijiie Chen, Jianlin Li, Chris Woan, Guojing Zhang